ELSEVIER

Chemical Geology 225 (2006) 189–212

CHEMICAL GEOLOGY
INCLUDING
ISOTOPE GEOSCIENCE

www.elsevier.com/locate/chemgeo

Dual-thermodynamic estimation of stoichiometry and stability of solid solution end members in aqueous–solid solution systems

D.A. Kulik *

Nuclear Energy and Safety Research Department, Laboratory for Waste Management, Paul Scherrer Institute, CH-5232 Villigen PSI, Switzerland

Accepted 16 August 2005

This paper is dedicated in memoriam to Professor Igor K. Karpov (1932–2005) — a brilliant geochemist, a pioneer in computer-aided (geo)chemical modeling, and a creator of the convex-programming GEM method based on the "dual thermodynamics" ideas.

Abstract

The dual-thermodynamic (DualTh) approach is shown to provide a useful alternative to other methods in: (i) forward modelling of equilibrium speciation, activities, and element partitioning in a heterogeneous system involving several variable-composition phases, such as the aqueous–solid solution system; (ii) estimation of interaction parameters of a non-ideal mixing model from known bulk compositions of coexisting aqueous and solid-solution phases; and (iii) retrieval of unknown stoichiometries and apparent standard chemical potentials of trace solid-solution end-members. Inverse-modelling tasks (ii) and (iii) can be performed when the solid solution of interest is shown experimentally to co-exist with the aqueous phase either in the equilibrium or at the minimum stoichiometric saturation state.

DualTh calculations exploit the ability of Gibbs energy minimisation (GEM) algorithms to find simultaneously two numerical solutions of the isobaric–isothermal chemical equilibrium speciation problem: (1) *primal* solution x — a vector of amounts of components (species) in phases; and (2) *dual* solution u — a vector of chemical potentials of stoichiometry units (usually chemical elements and charge). Conversely, the chemical potential of a phase component can be found in two complementary ways: (i) *primal* via its standard-state potential, concentration and activity coefficient (the latter two are functions of the x vector); and (ii) *dual* through its formula stoichiometry multiplied by the u vector. The DualTh methods compare primal and dual values of the chemical potential in simple and straightforward equations that can be easily computed in a spreadsheet, or implemented in GEM geochemical modelling codes.

Keywords: Aqueous system; Solid solutions; Mixing models; Equilibrium partitioning; Stoichiometric saturation; Gibbs energy minimization

1. Introduction

Many environmental contaminants can be immobilized by solid solution formation. However, the data on thermodynamic properties of solid solutions are still scarce because it is not easy to retrieve them unequivocally from the experimental information. This contribution summarizes the dual-thermodynamic (DualTh) methods that can be helpful in determining unknown solubility products of pure end-members or non-ideal mixing parameters.

DualTh calculations use the ability of Gibbs energy minimisation (GEM) convex programming algorithms (Karpov et al., 1997) to find two numerical solutions of the isobaric–isothermal chemical equilibrium speciation problem. The *primal* solution x is a vector of amounts of chemical species (*dependent components*, grouped

* Tel.: +41 56 3104742; fax: +41 56 3102821.
E-mail address: dmitrii.kulik@psi.ch.

0009-2541/$ - see front matter © 2005 Elsevier B.V. All rights reserved.
doi:10.1016/j.chemgeo.2005.08.014

into phases). The *dual* solution u is a vector of chemical potentials of stoichiometry units (independent components, usually chemical elements and charge). Accordingly, there are two possibilities of computing the chemical potential of any component at equilibrium: (1) *primal* via the standard-state potential, concentration and activity coefficient (the latter two are functions of the x vector); and (2) *dual* through the formula stoichiometry multiplied by the u vector.

The complementary primal and dual chemical potentials are connected via the necessary and sufficient conditions of equilibrium in Karpov–Kuhn–Tucker formulation (Karpov et al., 1997, 2001). Based on the so-called duality theorem of mathematical programming (hence the "dual solution"), these conditions make the GEM algorithm capable of eliminating unstable components and phases from the mass balance. For all components of stable phases, primal and dual chemical potentials must be numerically equal. Hence, for an end-member of a solid solution phase known to be in equilibrium with the rest of (aquatic) system, the elements of dual-solution u vector and, thus, the dual chemical potential can be obtained from a GEM calculation *not including* this phase in the mass balance (Karpov et al., 2001).

This leads to the DualTh equations that simplify modelling of heterogeneous systems involving several variable-composition phases, such as aqueous–solid solution (AqSS) systems. As will be shown in this contribution, the DualTh approach also provides a useful alternative to Lippmann functions (cf.(Gamsjäger et al., 2000; Glynn, 2000)): (i) in computing the equilibrium partitioning between solid solutions, gas, and aqueous electrolyte, and retrieving activities and their functions such as pH or pe (Karpov et al., 2001)); (ii) in retrieving unknown stoichiometries and apparent standard chemical potentials of solid-solution minor end-members (Curti et al., 2005; Kulik and Kersten, 2002); and (iii) in estimating activity coefficients and/or parameters of the non-ideal mixing model from the known experimental bulk compositions of coexisting aqueous and solid-solution phases (Kulik et al., 2000). From experimental viewpoint, the DualTh concept requires that the compositions of coexisting aqueous and solid solutions were reported in detail sufficient to compute aqueous equilibria, to estimate the extent of reaction, and to obtain end-member mole fractions in the solid solution.

The DualTh is, of course, not the only available method for determining end-member solubility products or interaction parameters from the results of co-precipitation, re-crystallization, or dissolution experiments. Such retrieval has been done earlier using the least squares fitting, the "activity ratios", the Lippmann diagrams (see "Discussion" section), the "unified theory of solid solution solubility", and other methods. In comparison, the DualTh technique is quite straightforward in that all the details of aquatic equilibrium are packed only into one dual solution vector, which is then simply transferred onto the solid solution of interest.

As long as the aqueous thermodynamic model, regardless of its complexity, remains adequate for the (experimental) system, the dual solution vector can be applied to any set of possible solid solution end-member stoichiometries. Perhaps, this is the main advantage of DualTh calculations, which, in the case when many experiments at different solid phase compositions are available, can be enhanced by simple statistical procedures. The *statistical* DualTh method, for the first time systematically described in this contribution, can select *optimal* end-member stoichiometries together with the solubility products and their uncertainty intervals. Last, but not least, after the dual solution of the aqueous phase equilibrium is obtained with the GEM algorithm, the remaining calculations are simple and can be performed with an ordinary spreadsheet program. The whole statistical DualTh calculation can also be done using the DualTh module of GEMS-PSI package v.2.1 (Kulik et al., 2004, 2003).

First DualTh calculations in GEM forward and inverse modelling have been performed only for the equilibrium case, using the criterion of equality of chemical potential of a component in all co-existing phases. Later on, it became possible to apply the inverse DualTh calculations to solid solutions at the minimum stoichiometric saturation state using a different criterion formulated by Gamsjäger and Königsberger (Gamsjäger, 1985; Königsberger and Gamsjäger, 1992a). The GEM DualTh implementation of this idea is described below for the first time, illustrated by a numerical example for the Mg-calcite-aqueous system.

Other goals of this paper are: to provide a systematic outlook of DualTh techniques based on the GEM algorithm, in both forward and inverse modelling; to describe a statistical variant of inverse DualTh calculations; and to highlight the specifics of DualTh interpretation of the minor/trace solid solution end members in common host minerals such as calcite.

2. Methods

The Law of Mass Action (LMA) method (Bethke, 1996; Parkhurst and Appelo, 1999) and the GEM con-

vex programming approach (Karpov et al., 1997, 2001) are complementary. The latter (GEM) is suited better to compute AqSS equilibria that include two or more multi-component phases than the former (LMA) which usually considers only one multi-component phase (usually aqueous electrolyte) in the mass balance and cannot find the dual solution of the equilibrium chemical speciation problem.

2.1. Gibbs energy minimization

In GEM, total amounts of chemical elements and (zero) charge comprise the input bulk composition of the system (vector b). All stoichiometrically feasible *chemical species* are taken into the mass balance through their chemical formulae. A chemical species (*dependent component*) belongs to a single- or multi-component aqueous, gaseous, fluid, liquid, solid, or sorption phase. Stability of j-th chemical species at temperature T and pressure P of interest is defined by its input standard molar Gibbs energy function g_j^{o}. Activities and concentrations of dependent components are treated separately in each phase, taking into account the appropriate standard and reference states, concentration scales, and mixing models. Conversely, GEM algorithms can solve complex AqSS equilibria in a straightforward way, without supporting tools such as Lippmann functions (Glynn, 1991) required in LMA AqSS speciation models.

2.2. The GEM forward modeling problem

Forward modeling means here a calculation of (unknown) equilibrium phase assemblage and speciation in the system defined by T, P, bulk composition, thermodynamic data for dependent components belonging to the set L, and, optionally, parameters of mixing in multi-component phases. Solving this problem is equivalent to finding a vector of amounts of dependent components $x=\{x_j, j\in L\}$ such that

$$G(x)\Rightarrow\min \quad \text{subject to } Ax=b \tag{1}$$

where $b=\{b_i, i\in N\}$ is the input vector of amounts of independent components belonging to the set N; $A=\{a_{ij}, i\in N, j\in L\}$ is a matrix made of the formula stoichiometry coefficients of dependent components; and $G(x)$ is a total Gibbs energy function of the system

$$G(x)=\sum_j x_j \upsilon_j, \quad j\in L \tag{2}$$

In Eq. (2), υ_j is the normalized chemical potential of j-th dependent component, written in a simplified dimensionless form as:

$$\upsilon_j=\frac{g_j^o}{RT}+\ln C_j+\ln\gamma_j+\Xi, \quad j\in L \tag{3}$$

where g_j^{o} is the standard molar Gibbs energy function at temperature of interest (pressure dependence is omitted for simplicity); R is the universal gas constant; T is temperature (K); $C_j=f(x_j)$ is the concentration (mole fraction χ_j for a component of gas or solid solution phase, molality m_j for aqueous electrolyte species, and so on); γ_j is the activity coefficient of j-th dependent component in its respective phase (unity in a Raoultian ideal mixture). The conversion term Ξ depends on the chosen standard state, e.g., $\Xi=\ln P$ for gas phase components, $\Xi=1-\chi_{\mathrm{w}}$ for aqueous species (χ_{w} is the mole fraction of water), and $\Xi=0$ for solid solution end-members and single-component phases. Full expressions for υ_j and Ξ in aqueous and sorption phases can be found in (Karpov et al., 2001; Kulik, 2002). Activity coefficients γ_j (as functions of the phase composition) are calculated at each iteration of the GEM algorithm according to the mixing model chosen for each phase (see Section 2.2.2 for solid solutions).

The Interior Points Method (IPM) non-linear GEM algorithm finds simultaneously two vectors— *primal* $\hat{x}$ and *dual* u solutions of the problem (1)— using the necessary and sufficient conditions for equilibrium in the *Karpov–Kuhn–Tucker* formulation (Karpov et al., 1997)

$$\upsilon - A^{\mathrm{T}}u\geq 0;$$

$$A\hat{x}=b; \quad \hat{x}\geq 0;$$

$$\hat{x}^{\mathrm{T}}\left(\upsilon - A^{\mathrm{T}}u\right)=0 \tag{4a, b, c, d}$$

where $^{\mathrm{T}}$ is the transpose operator. Condition Eq. (4a), re-written with indices using Eq. (3),

$$\frac{g_j^o}{RT}+\ln C_j+\ln\gamma_j+\Xi-\sum_i a_{ij}u_i\geq 0, \quad j\in L,\ i\in N \tag{5}$$

implies that for any j-th species present at some equilibrium concentration C_j in its phase, the *primal* chemical potential υ_j numerically equals the *dual* chemical potential

$$\eta_j=\sum_i a_{ij}u_i, \ j\in L, \ i\in N \tag{6}$$

From the duality theorem it follows that, at equilibrium, the total Gibbs energy of the system is $G(\hat{x})=G(u)$, where $G(\hat{x}) = \sum_j \hat{x}_j \upsilon_j$ (Eq. (1)) and $G(u) = \sum_i b_i u_i,\ i \in N$. Hence, the GEM dual solution u_j values (Lagrange multipliers) are chemical potentials of independent components in the equilibrium state of interest. The condition of complementary slackness (4d) complements conditions (4a) or 5 in a sense of selecting stable components (for which the equality in Eq. (5) can be achieved at a positive amount x_j or concentration C_j) from the unstable ones (for which the equality in Eq. (5) cannot be reached and zero amount x_j must be assigned). Conditions (4a, 4c, 4d) have also been extended for the case when the sought-for amounts x_j of some metastable species are constrained from below and/or above to model "partial equilibrium" states (Karpov et al., 2001). In this work, GEM calculations were performed using the GEMS-PSI v.2.1 code (Kulik et al., 2004) with built-in Nagra/PSI data base (Hummel et al., 2002).

2.3. DualTh calculations in forward modeling

For any species in any phase present at equilibrium, the first Karpov–Kuhn–Tucker condition (Eq. (4a)) can be combined with Eqs. (3) and (6) into a generic DualTh equation $\eta_j=\upsilon_j$, or

$$\sum_i a_{ij} u_i = \frac{g_j^o}{RT} + \ln C_j + \ln \gamma_j + \Xi. \tag{7}$$

In the forward speciation modelling, equations derived from (7) are internally used (in GEM-Selektor code) to calculate: (i) activities of gaseous, aqueous, solid-solution and sorption species, (ii) activity functions such as pH, pe; and (iii) saturation indices of single-component condensed phases. The activity of j-th dependent component is understood here as a *relative activity* $a_j=r_j\gamma_j$ from the IUPAC definition of chemical potential

$$\mu_j = \mu_j^o + RT\ln a_j = \mu_j^o + RT\ln r_j + RT\ln\gamma_j \tag{8}$$

where r_j stands for a *relative content*. Comparison with Eq. (3) shows that r_j is related to concentration as $\ln r_j=\ln C_j+\Xi$. According to Eqs. (6) and (8), the DualTh equation for calculation of activity of any component in any multi-component phase present at equilibrium is:

$$\ln a_j = \sum_i a_{ij} u_i - \frac{g_j^o}{RT}, \quad j \in L, \quad i \in N \tag{9}$$

The usual calculation of activity is $\ln a_j = \ln C_j + \Xi + \ln\gamma_j$. As both C_j and γ_j are functions of the primal solution x vector, thus computed activities are subject to some numerical limitations. For instance, neither LMA nor GEM algorithms can consider amounts (concentrations) below 10^{-18} to 10^{-20} moles; smaller values are automatically zeroed off for convergence reasons. For such "zeroed-off" species, Eq. (9) is the only way to compute the activity in GEM algorithm, applicable also to stoichiometrically feasible minor species not even included into the mass balance, for instance, the "aqueous electron" e_{AQ} — a hypothetical species used in the definition of pe — a measure of redox potential. For the e_{AQ} species (formula charge $Z=-1$ and $g^o=0$ by convention), Eq. (9) takes the form $\ln a_e = -1 \cdot u_{Charge}$; defining $pe=-\log_{10} a_e$, one gets

$$pe = -\frac{1}{\ln 10}\left(-u_{Charge}\right). \tag{10}$$

Using the fundamental relation $pe \cdot \ln 10 \cdot RT = F \cdot Eh$ (F is the Faraday constant), pe can be converted into Eh (in Volts)

$$Eh = \frac{R}{F} \cdot T \cdot u_{Charge} \tag{11}$$

In a similar way, $pH=-\log_{10} a_{H^+}$ can be calculated for any aquatic system, even if the aqueous H^+ species is not explicitly included into the mass balance

$$pH = -\frac{1}{\ln 10}\left(u_H + u_{Charge}\right) \tag{12}$$

In this equation, consistent with the electrochemical convention $g^o(H^+)=0$ at any T and P, the activity coefficient of H^+ ion is not required at all. Eq. (12) always yields a robust numerical value of pH, even in very alkaline systems, where the H^+ molality drops below 10^{-12}.

In the case of fugacity f_j of a gaseous component, e.g., O_2 or CO_2, the relative activity can be defined as $\mu_j - \mu_j^o = RT\ln a_j = RT\left(\ln f_j - \ln f^o\right)$ (Anderson and Crerar, 1993). Because the standard-state fugacity $f^o=1$ bar for any gaseous component, its activity a_j (dimensionless) is numerically equal to the fugacity f_j. Hence, Eq. (9) can be used for computing a gas fugacity value, even if the gas mixture is not present in a positive amount at equilibrium, or it has not been included into the system definition. For example, the fugacity of ideal CO_2 gas at $T=25$ °C in any system containing C and O can be found using the DualTh equation:

$$\log_{10} f_{CO_2,g} = \frac{1}{ln 10}\left[u_C + 2u_O - (-159.1)\right] \tag{13}$$

where −159.1 is the normalized (divided by RT=2479 J mol^{-1}) standard molar Gibbs energy of CO_2 gas at 25 °C.

There are two cases of application of Eq. (9) to condensed (solid) phases. If a mixture end-member is present in equilibrium in a positive amount then Eq. (9) directly yields its activity. For instance, for the barite end-member in (Ba,Sr)SO_4 solid solution at 25 °C and 1 bar,

$$\log_{10} a_{\mathrm{Barite,s}} = \frac{1}{\ln 10}\left[u_{\mathrm{Ba}} + u_{\mathrm{S}} + 4u_{\mathrm{O}} - (-549.48)\right].$$

For a single-component solid, one can find from Eq. (9) the value of saturation index (SI) defined as

$$\Omega_{\mathrm{s}} = \log_{10}\frac{Q_r}{K_{\mathrm{eq}}} = \frac{1}{\ln 10}\left(\ln Q_{\mathrm{r}} - \ln K_{\mathrm{eq}}\right) \quad (14)$$

where K_{eq} is the equilibrium constant, and Q_{r} is the dissolution reaction quotient (Langmuir, 1997). For example, taking calcite $CaCO_3$ as a single-component phase, Eq. (9) leads to

$$\Omega_{\mathrm{Calcite,s}} = \frac{1}{\ln 10}\left[u_{\mathrm{Ca}} + u_{\mathrm{C}} + 3u_{\mathrm{O}} - (-455.5)\right]. \quad (15)$$

At equilibrium, SI is (numerically) zero. The statement that the equation like (15) gives the SI for a pure phase can be proved as shown in Appendix A. In GEMS-PSI code, negative values of SI are always computed for unstable pure solid phases eliminated from the mass balance; positive SI values can be obtained only for solids with the amount x_j kinetically constrained from above (Karpov et al., 2001). Eqs. like (15) apply also to stoichiometrically feasible single-component solids not included into the mass balance. Note that the DualTh SI calculation involves neither reactions nor ion activity or solubility products, as the usage of the classic Eq. (14) would require.

2.4. Inverse modeling in AqSS equilibrium

Inverse thermodynamic modeling can be performed when part of the output amount vector x or some functions of it are independently known (experimental fugacities, bulk compositions, concentrations of ions, electrode potentials, etc.), but part of the input data (b, T, P, g^{o}, parameters of mixing) are missing. The goal is to obtain (or refine) values of unknown or uncertain input parameters. At earlier times, the recognition of inverse problems has led to development of specialized codes such as FITEQL (Herbelin and Westall, 1996) which could fit chemical speciation models to the experimental data using the least-squares algorithms. Karpov et al. (1999) suggested another approach to solve inverse problems in a broader "uncertainty space" concept of geochemical modeling under uncertainty of input data.

The present contribution is intended not to provide an overview of inverse modeling methods, but, rather, to focus on three specific cases related to AqSS systems: (i) determination of unknown standard chemical potentials and solubility products K_{SP} of end members with known activity coefficients γ; (ii) finding unknown activity coefficients (and parameters of non-ideal mixing) at known end-member K_{SP}; and (iii) finding stoichiometries with apparent standard chemical potentials of minor and trace end-members when neither K_{SP} nor γ are known separately. All three tasks can be efficiently solved using GEM DualTh calculations.

For a j-th solid solution end member, the generic Eq. (7) can be re-arranged as

$$\mu_j^{\mathrm{o}} + RT\ln\gamma_j = \mu_j^{(u)} - RT\ln\chi_j \quad (16)$$

where $\mu_j^{\mathrm{o}}=g_j^{\mathrm{o}}$, $\mu_j^{(u)}=RT\eta_j$, η_j is defined by Eq. (6), γ_j is the activity coefficient, and χ_j is the (independently known) mole fraction of end-member stoichiometry in the solid solution phase. In equilibrium, the criterion behind Eq. (16) is that the chemical potential of an independent component is the same in the solid solution and the co-existing aqueous phase. Hence, the value $\mu_j^{(u)}$ can be obtained by solving a GEM problem (Eq. (1)) for the part of the system without the solid solution of interest, given that the bulk composition of that part can be retrieved from experimental data. Then, one unknown parameter on the left-hand side of Eq. (16) can be immediately calculated. This idea (in a more formal notation) has been first expressed by Karpov et al. (2001) and has already been used in several GEM applications (Kulik et al., 2000; Kulik and Kersten, 2002; Curti et al., 2005).

2.4.1. Retrieval of end-member standard molar Gibbs energy and solubility product

The DualTh equation for this case is obtained by further re-arranging Eq. (16):

$$g_j^{o} = \mu_j^{(u)} - RT\left(\ln\chi_j + \ln\gamma_j\right). \quad (17)$$

Eq. (17) implies that the bulk composition (to calculate χ_j) and the mixing model parameters (to calculate γ_j) of the solid solution are known. In some ionic structures (carbonates, sulfates), the binary interaction parameters can be semi-empirically predicted (Urusov, 1975; Lippmann, 1980; Glynn, 2000; Becker et al.,

2000). Further development of atomistic modeling techniques (Vinograd, 2001; Becker and Pollok, 2002) may lead to the prediction of mixing properties also in oxide and silicate systems. In the worst case of ill-defined structure, a formally ideal mixing model can be applied (Kulik and Kersten, 2001). Stoichiometries of all end-members must be known for the calculation of χ_j from the solid bulk composition. This may be a non-trivial task for the reciprocal solid solution (Wood and Nicholls, 1978).

The retrieved value of end-member g_j^o can be converted into an equilibrium constant of the reaction, for instance solubility product K_{SP}, using the relation $\log_{10}K = -\dfrac{\Delta_r G^o}{RT\ln 10}$. Other g^o values needed to compute $\Delta_r G^o$ can be found in chemical thermodynamic data bases.

2.4.2. Retrieval of activity coefficients and mixing parameters

The DualTh equation for this case results from another re-arrangement of Eq. (16)

$$\ln\gamma_j = \frac{\mu_j^{(u)} - g_j^o}{RT} - \ln\chi_j \tag{18}$$

It is implied that the end-member stoichiometry and g_j^o value are known, and the mole fraction χ_j can be calculated from the known bulk composition of solid solution. Further conversion of the estimated $\ln\gamma_j$ depends on the number of available experiments at different solid compositions, and on the non-ideal mixing model of choice. Among these models, the Guggenheim or the Redlich–Kister, and the Margules models are widely used (Glynn, 1991, 2000; Anderson and Crerar, 1993; Nordstrom and Munoz, 1994). The Redlich–Kister model (for binary solutions) is based on a Guggenheim power-series expression for the excess Gibbs energy of mixing G^E

$$G^E = RT(\chi_1\ln\gamma_1 + \chi_2\ln\gamma_2) = RT\chi_1\chi_2\sum_r \alpha_r(\chi_1-\chi_2)^r \tag{19}$$

where the coefficients α_r are called interaction parameters, which, in general, depend on temperature and pressure. The activity coefficients corresponding to Eq. (19) are expressed as

$$\ln\gamma_1 = \chi_2^2(\alpha_0 + \alpha_1(3\chi_1-\chi_2) + \alpha_2(\chi_1-\chi_2)(5\chi_1-\chi_2) + \ldots) \tag{20a}$$

$$\ln\gamma_2 = \chi_1^2(\alpha_0 - \alpha_1(3\chi_2-\chi_1) + \alpha_2(\chi_2-\chi_1)(5\chi_2-\chi_1) + \ldots) \tag{20b}$$

Two parameters α_0 and α_1 (subregular model), or even a single parameter α_0 (regular model), are usually sufficient in binary systems; the corresponding equations for ternary and higher-order systems are available in the literature. Some theoretical low-temperature binary systems may require more parameters of Eq. (19) (Prieto et al., 2000). The subregular model is equivalent to the asymmetric Margules model in the Thompson–Waldbaum notation

$$G^E = RT(\chi_1\ln\gamma_1 + \chi_2\ln\gamma_2) = \chi_1\chi_2(W_{12}\chi_2 + W_{21}\chi_1) \tag{21}$$

with the parameters

$$W_{12} = RT(\alpha_0-\alpha_1); W_{21} = RT(\alpha_0+\alpha_1) \tag{22a, b}$$

and the activity coefficients

$$RT\ln\gamma_1 = (2W_{21}-W_{12})\chi_2^2 + 2(W_{12}-W_{21})\chi_2^3 \tag{23a}$$

$$RT\ln\gamma_2 = (2W_{12}-W_{21})\chi_1^2 + 2(W_{21}-W_{12})\chi_1^3. \tag{23b}$$

In the symmetric Margules model, $W_{12}=W_{21}=W_G$ and $W_G=RT\alpha_0$, i.e., both Redlich–Kister and Margules models reduce to the same (regular) type of expression.

In equilibrium between the aqueous solution and a binary solid solution, two activity coefficients γ_1 and γ_2 (for each end member) can be found using Eq. (18) even for a single experimental point. Since mole fractions χ_1 and χ_2 of both end members are known, the system of Eqs. (20a,b) can be solved algebraically to find two parameters α_0 and α_1

$$\alpha_0 = \frac{1}{2}\left[\frac{\ln\gamma_1}{\chi_2^2}(3\chi_2-\chi_1) + \frac{\ln\gamma_2}{\chi_1^2}(3\chi_1-\chi_2)\right];$$
$$\alpha_1 = \frac{1}{2}\left(\frac{\ln\gamma_1}{\chi_2^2} - \frac{\ln\gamma_2}{\chi_1^2}\right). \tag{24a, b}$$

Alternatively, the system of Eqs. (23a,b) can be solved for Margules parameters W_{12} and W_{21}

$$W_{12} = RT\left[\frac{2\ln\gamma_2}{\chi_1} + \frac{\ln\gamma_1}{\chi_2^2}(\chi_2-\chi_1)\right];$$
$$W_{21} = RT\left[\frac{2\ln\gamma_1}{\chi_2} + \frac{\ln\gamma_2}{\chi_1^2}(\chi_1-\chi_2)\right]. \tag{25a, b}$$

Consistency of the above expressions for Redlich–Kister and Margules parameters can be easily checked by substituting Eqs. (24a,b) and (25a,b) into Eqs. (22a,b). Clearly, if the calculated $\alpha_1 \approx 0$, or $W_{12} \approx W_{21}$, the regular binary model should be used instead, with a parameter

$$\alpha_0 = \frac{W_G}{RT} = \frac{1}{2}\left(\frac{\ln\gamma_1}{\chi_2^2} + \frac{\ln\gamma_2}{\chi_1^2}\right) \tag{26}$$

Having a single equilibrium point, it is hardly possible to estimate the errors of thus calculated binary interaction parameters. For each of several $n(Q)$ experiments performed at different solid phase compositions, it is possible to calculate activity coefficients of both end members $\gamma_{1,q}$ and $\gamma_{2,q}$ using the DualTh Eq. (18), and estimate interaction parameters using Eqs. (24a,b) or (25a,b). From thus obtained $n(Q)$ values of a parameter, its average and standard deviation can be found directly, avoiding the least-squares fitting.

2.4.3. Retrieval of apparent molar Gibbs energy for a trace end-member

Incorporation of hazardous trace elements into solid solutions is an important topic in waste geochemistry. Especially in the case of heterovalent substitutions (e.g., Eu^{III} in $CaCO_3$), the trace end-member may not exist as a pure substance, and a hypothetical stoichiometry of unknown stability may have to be tested (Curti et al., 2005). If the structural mechanism of incorporation is not yet known then the trace end member activity coefficient cannot be predicted. Although both parameters on the left-hand side of Eq. (16) may be unknown, their sum — the apparent molar Gibbs energy $g^*_{\mathrm{Tr}} = g^{\mathrm{o}}_{\mathrm{Tr}} + RT\ln\gamma_{\mathrm{Tr}}$— can still be found:

$$g^*_{\mathrm{Tr}} = \mu^{(u)}_{\mathrm{Tr}} - RT\ln\chi_{\mathrm{Tr}} \tag{27}$$

At trace mole fraction ($\chi_{\mathrm{Tr}} < 10^{-3}$), the activity coefficient γ_{Tr} can be taken constant even in a strongly non-ideal binary mixture. This is seen from Eqs. (20a,b) or (23a,b) if one takes the end-member 1 as trace and the end-member 2 as major ($\chi_2 > 0.999$). Therefore, the g^*_{Tr} estimate should have the same value if calculated with Eq. (27) from multiple experiments along the trace metal incorporation isotherm. The non-ideality would not change the isotherm slope, just would shift its position up or down relative to the ideal isotherm.

2.4.4. Algorithm of the single DualTh calculation at equilibrium

The main DualTh criterion at equilibrium consists in equality of chemical potentials of independent components in all co-existing phases. The DualTh calculation (in particular, for the AqSS system) is performed using a simple algorithm after (Karpov et al., 2001):

1. Define a ***basis sub-system***, i.e., a set $L^{(\mathrm{BS})}$ of chemical species belonging to the aqueous phase and/or all other equilibrium phases with known g^{o} and γ for all components, but excluding any dependent components having these properties unknown.
2. Calculate the equilibrium state in the basis sub-system only from its known bulk composition $b^{(\mathrm{BS})}$ using the GEM algorithm to obtain the dual solution vector $u^{(\mathrm{BS})}$ of chemical potentials of independent components.
3. Define a ***non-basis sub-system***— a set $L^{(\mathrm{NS})}$ of solid-solution end-members of interest, some with unknown g^{o}_j or γ_j, $j \in L^{(\mathrm{NS})}$, $n(L^{(\mathrm{NS})}) \geq 2$. Include also major end-members.
4. From the known bulk composition $b^{(\mathrm{NS})}$ of the non-basis sub-system, calculate mole fractions χ_j, $j \in L^{(\mathrm{NS})}$ for all end-member stoichiometries from the set $L^{(\mathrm{NS})}$.
5. For each component from the non-basis sub-system: if the activity coefficient γ_j is known then use Eq. (17) to obtain a g^{o}_j estimate; if g^{o}_j is known then use Eq. (18) to retrieve the activity coefficient γ_j; and for a hypothetical trace end-member, use Eq. (27) to calculate the apparent molar Gibbs energy g^*_j.

Calculations at steps 4 and 5 are simple and can be done on a spreadsheet after computing all the basis subsystem equilibria using the GEM code at step 2.

2.5. Inverse modeling at minimum stoichiometric saturation

At low temperatures, if the formation of secondary solid phases is kinetically inhibited, some solid solutions appear to dissolve congruently, as fixed-composition solids. This process slows down with time to a metastable state of stoichiometric saturation (Glynn and Reardon, 1990; Königsberger and Gamsjäger, 1992a; Glynn, 2000), the relevance of which is still debated (Gamsjäger et al., 2000). It appears that sparingly soluble solid solutions with similar end member solubility products are prone to the stoichiometric saturation at room temperatures and experimental times of about a week (Gamsjäger, 1985). On a Lippmann diagram, the minimum stoichiometric saturation states fall to the "equal-G" curve EGC (Königsberger and Gamsjäger, 1992a; Glynn, 2000), the criteria of which are: (i) the equality of end-member mole fractions, and (ii) the equality of integral molar Gibbs energies of mixture in both solid and in aqueous phases:

$$\chi^{(\mathrm{BS})}_j = \chi^{(\mathrm{NS})}_j = \chi_j; \tag{28a}$$

$$G^{(\mathrm{NS})}_{\mathrm{SS}} = \sum_i \mu^{(\mathrm{NS})}_j \chi_j = G^{(\mathrm{BS})}_{\mathrm{SS}} = \sum_j \mu^{(\mathrm{BS})}_j \chi_j \tag{28b}$$

where the superscript $^{(\mathrm{NS})}$ denotes the value obtained for the non-basis sub-system (solid solution), and the

superscript $^{(BS)}$ marks the value derived from the equilibrium in the basis sub-system (aqueous electrolyte) alone. There is no true equilibrium between the two phases, thus $\mu_j^{(NS)}$ is not necessary equal to $\mu_j^{(BS)}$. In all cases below, the bulk composition of solid solution (NS) and, hence, mole fractions of end-members χ_j, are assumed to be experimentally known.

2.5.1. Retrieval of end-member standard molar Gibbs energy

If the mixing model for the solid is known, Eq. (28b) can be re-arranged for estimating the g^o value of one k-th end-member:

$$g_k^o = \frac{G_{SS}^{(BS)} - G^E}{\chi_k} - \frac{RT}{\chi_k}\sum_j \chi_j \ln\chi_j - \frac{1}{\chi_k}\sum_{j\neq k}\chi_j g_j^o. \tag{29}$$

Here, G^E is the known molar excess Gibbs energy (Eqs. (19) or (21)); the simplest cases are $G^E=0$ for the Raoultian ideal mixing, and $G^E=W_G\chi_1\chi_2$ for the regular binary model.

2.5.2. Retrieval of the excess Gibbs energy of mixing

If standard molar Gibbs energies of all solid solution end members are known then the excess Gibbs energy of mixing can be retrieved by re-arranging Eq. (28b)

$$G^E = G_{SS}^{(BS)} - RT\sum_j \chi_j \ln\chi_j - \sum_j \chi_j g_j^o \tag{30}$$

keeping in mind that

$$\sum_j \chi_j\mu_j = G_{SS} = G_{SS}^o + G^{Id} + G^E$$
$$= \sum_i \chi_j g_j^o + RT\sum_j \chi_j\ln\chi_j + RT\sum_j \chi_j\ln\gamma_j.$$

Further on, the interaction parameters can be found from Eqs. (19) or (21), perhaps, using the least squares fitting if many experiments are available. In the case of regular model, only one interaction parameter (instead of two at equilibrium) can be found from a single experiment:

$$W_G = \frac{G^E}{\chi_1\chi_2} \tag{31}$$

2.6. Statistical DualTh calculations in inverse modeling

From a single DualTh calculation, neither the uncertainty interval of the retrieved g_j*, g_j^o or α_0 value can be found, nor the criteria for selection of the optimal end-member stoichiometry can be constructed. However, both tasks can be done having the data of multiple AqSS partitioning experiments at different compositions (e.g., an isotherm). Using the statistical DualTh approach, Kulik and Kersten (2002) selected the Zn-containing end member stoichiometry using solubility data on Zn-doped calcium silicate hydrate (C–S–H). Curti et al. (2005) applied the statistical DualTh in their study of Eu^{III} incorporation in calcite. Most statistical DualTh calculations, for the first time systematically described in this paper, are now being implemented in a DualTh module of GEM-Selektor code package (Kulik et al., 2004). The data flow chart of statistical DualTh calculations is shown on Fig. 1.

Let Q be a set of $n(Q)>2$ AqSS partitioning experiments performed at known T and P, and in each q-th experiment, the basis sub-system (BS, aqueous solution) is shown to be either in equilibrium or in minimum stoichiometric saturation with the non-basis sub-system (NS, solid solution). For simplicity reasons, we assume T and P the same for all experiments.

Input data consists of two matrices: $B^{(BS)}$ composed of $n(Q)$ non-equal bulk composition vectors for basis sub-systems (taken as columns)

$$B^{(BS)} = \left\|b_{qi}^{(BS)}\right\|, \quad q\in Q,\ i\in N \tag{32}$$

and $B^{(NS)}$ containing $n(Q)$ bulk composition vectors for non-basis sub-systems

$$B^{(NS)} = \left\|b_{qi}^{(NS)}\right\|, \quad q\in Q,\ i\in N. \tag{33}$$

In each matrix, columns refer to independent components (chemical elements).

Step 1 consists in performing a series of $n(Q)$ GEM calculations of equilibria in each basis sub-system, resulting in a dual solution matrix $U^{(BS)}$:

$$U^{(BS)} = \left\|u_{qi}^{(BS)}\right\|, \quad q\in Q,\ i\in N. \tag{34}$$

Each row in this matrix is a dual solution vector for the q-th experiment.

At **step 2**, a set M of $n(M)\geq 2$ candidate end-member stoichiometries for the non-basis sub-system is defined. Each formula expands into a row in the stoichiometry matrix

$$A^{(NS)} = \left\|a_{mi}^{(NS)}\right\|, \quad m\in M,\ i\in N. \tag{35}$$

The set M must contain one or more subsets Π_m, $n(\Pi_m)<n(M)$ of solid solution end members (indexed with p) that complement any m-th ($m\in M\setminus\Pi_m$) end member of interest to a full (binary, ternary, ...) solid solution model needed to solve each q-th solid bulk

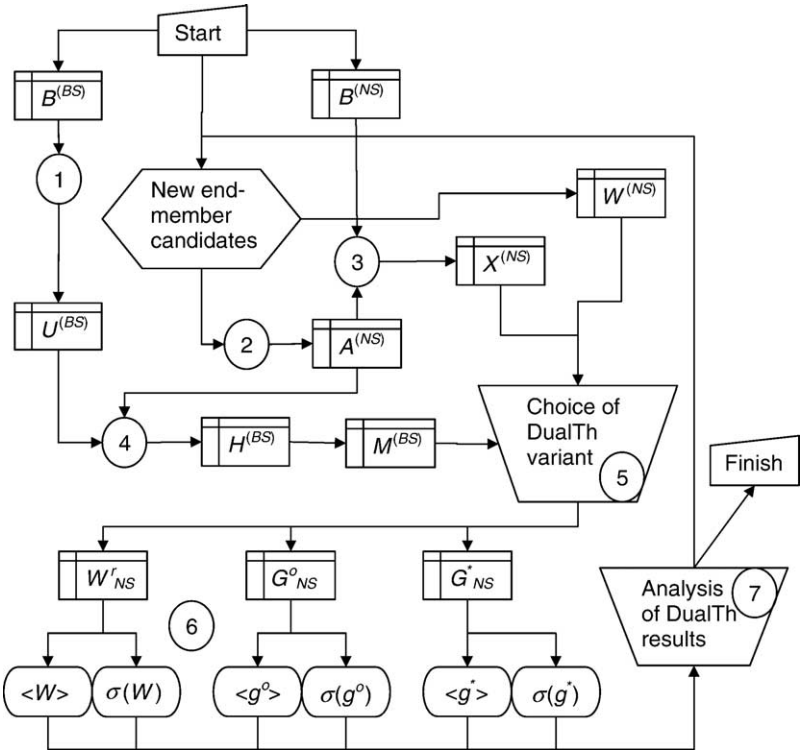

Fig. 1. Data flow chart of statistical DualTh calculations. Symbols in the boxes for data tables and vectors correspond to Eqs. (32)–(49). Digits in circles refer to the algorithmic steps described in the text. <*X*> means "average *X*".

composition for the mole fraction(s) χ_{qm} of end members. The solid solution end-member candidates can be chosen in many ways — as existing pure solids for the element of interest, from the phase diagram topology, or from the consideration of substitution mechanisms. The number of alternative stoichiometries should be kept small, and their formulae— as simple as possible.

Step 3 consists in the calculation of mole fractions $\chi_{qm}^{(\mathrm{NS})}$ of each of $n(M)$ end-member stoichiometries for each of $n(Q)$ experiments in the non-basis sub-system, forming a matrix

$$X^{(\mathrm{NS})} = \left|\left|\chi_{qm}^{(\mathrm{NS})}\right|\right|, \quad q\in Q,\ q\in M \tag{36}$$

in which rows correspond to the experiments, and columns- to end-member candidates. For the q-th experiment, mole fractions $\chi_{qm}^{(\mathrm{NS})}$ are subject to the mole balance constraints:

$$X_q \sum_m a_{mi}^{(\mathrm{NS})}\chi_{qm}^{(\mathrm{NS})} + X_q \sum_p a_{pi}^{(\mathrm{NS})}\chi_{qp}^{(\mathrm{NS})} = b_{iq}^{(\mathrm{NS})},$$
$$p\in\Pi_m,\ i\in N,\ m\in M\diagdown\Pi_m \tag{37}$$

where X_q is the (unknown) amount of the solid solution with m-th end-member candidate of interest, and $\chi_{qp}^{(\mathrm{NS})}$ is the (unknown) mole fraction of p-th complementary end member. Eq. (37) defines a system of $n(N)$ balance equations with $n(\Pi_m)+n(M\backslash\Pi_m)+1$ unknowns ($\chi_{qm}^{(\mathrm{NS})}$, $\chi_{qp}^{(\mathrm{NS})}$ and X_q). If $n(N)\geq n(\Pi_m)+n(M\backslash\Pi_m)$ (one mole fraction is not independent and can be calculated from others), the system of Eq. (37) can be solved algebraically to obtain mole fractions $\chi_{qm}^{(\mathrm{NS})}$, $\chi_{qp}^{(\mathrm{NS})}$. We assume here that $\chi_{qm}^{(\mathrm{NS})}$ values can be calculated for all experiments and end-member stoichiometries of interest.

At **step 4**, GEM dual solution matrix $U^{(\mathrm{BS})}$ (Eq. (34)) with end-member stoichiometry matrix $A^{(\mathrm{NS})}$ (Eq. (35)) are used in finding dual chemical potentials of end-member stoichiometries

$$H^{(\mathrm{BS})} = ||\eta_{qm}^{(\mathrm{BS})}||, \quad q\in Q,\ m\in M \tag{38}$$

by the matrix multiplication:

$$H^{(\mathrm{BS})} = \left(A^{(\mathrm{NS})}\right)^{\mathrm{T}} U^{(\mathrm{BS})} \tag{39a}$$

or, in the index notation,

$$\eta_{qm}^{(\mathrm{BS})} = \sum_i a_{mi}^{(\mathrm{NS})} u_{qi}^{(\mathrm{BS})}, \quad q\in Q,\ m\in M,\ i\in N. \tag{39b}$$

The matrix of normalized dual chemical potentials $H^{(BS)}$ can be converted into the matrix of chemical potentials $M^{(BS)}$ using a scalar multiplication by the RT factor:

$$M^{(BS)} = ||\mu_{qm}^{(BS)}|| = RT \cdot ||\eta_{qm}^{(BS)}||, \quad q \in Q,\ m \in M. \quad (40)$$

Step 5 generalizes the DualTh calculations given by Eqs. (17), (18) or (27) for the equilibrium case, or those by Eqs. (29)–(31) for the minimum stoichiometric saturation case by introducing the proper indexation for each q-th experiment and each m-th end-member. At equilibrium, the matrix of dual chemical potentials of end members $M^{(NS)}$ is the same as the matrix of chemical potentials in the basic sub-system $M^{(BS)}$. Hence, Eq. (17) takes the form:

$$g_{qm}^{o} = \mu_{qm}^{(BS)} - RT\left(\ln\chi_{qm}^{(NS)} + \ln\gamma_{qm}^{(NS)}\right), \quad q \in Q,\ m \in M \quad (41)$$

where $\gamma_{qm}^{(NS)}$ is the activity coefficient found from the mole fractions $\chi_{qm}^{(NS)}$ and $\chi_{qp}^{(NS)}$, and from known mixing model. For the minimum stoichiometric saturation, Eq. (30) can be re-written as

$$G_q^E = G_{SS,q}^{(BS)} - RT\sum_m \chi_{qm}\ln\chi_{qm} - \sum_m \chi_{qm} g_m^o, \quad q \in Q,\ m \in M \quad (42)$$

where g_m^o stands for the known standard molar Gibbs energy of m-th end-member candidate. For instance, using Eq. (31), the Margules parameter for a regular solution of end-members 1 and 2 in a q-th experiment can be found as:

$$W_{G,q} = \frac{1}{\chi_{q,1}\chi_{q,2}} G_{SS,q}^{(BS)} - \frac{1}{\chi_{q,2}}\left(g_1^o + RT\ln\chi_{q,1}\right) - \frac{1}{\chi_{q,1}}\left(g_2^o + RT\ln\chi_{q,2}\right). \quad (43)$$

Whatever the DualTh equation used, the Step 5 results either in a matrix G_{NS}^o (G_{NS}^*) containing g_{qm}^o (g_{qm}^*) values for $n(M)$ end-members in $n(Q)$ experiments, or in a matrix $W_{NS}^{(r)}$ of the estimated interaction parameters. Formally,

$$G_{NS}^o = \left\| g_{qm}^o \right\|, \quad q \in Q,\ m \in M \quad (44)$$

$$G_{NS}^* = \left\| g_{qm}^* \right\|, \quad q \in Q,\ m \in M \quad (45)$$

$$W_{NS}^{(r)} = \left\| W_{qr} \right\|, \quad q \in Q,\ r \in \vartheta \quad (46)$$

where ϑ denotes the set of $n(\vartheta)$ interaction parameters (1 for symmetric binary, 2 for asymmetric binary, 4 for symmetric ternary, and so on). It is important that $n(Q) \geq 2n(\vartheta)$ in equilibrium with a binary solid solution, and $n(Q) > n(\vartheta)$ at the stoichiometric saturation.

At **step 6**, the statistical analysis of the columns of either of matrices (Eqs. (44)–(46)) is performed. In the simplest case, means and standard deviations over each column are calculated. For the matrix G_{NS}^o (Eq. (44)), this results in a vector-row of mean values

$$\bar{g}^o = \left\{\bar{g}_m^o\right\}, \quad m \in M \quad , \quad (47a)$$

and a vector-row of standard deviation values

$$\sigma(g^o) = \left\{\sigma\left(g_m^o\right)\right\}, \quad m \in M \quad (47b)$$

where

$$\bar{g}_m^o = \frac{1}{n(Q)}\sum_q g_{qm}^o, \quad q \in Q,\ m \in M;$$

$$\sigma\left(g_m^o\right) = \sqrt{\frac{1}{n(Q)}\sum_q \left(g_{qm}^o - \bar{g}_{qm}^o\right)^2}, \quad q \in Q,\ m \in M.$$

For the matrix G_{NS}^* (Eq. (45)), the mean and standard deviation vectors are

$$\bar{g}^* = \bar{g}_m^*, \ \ m \in M;\ \ \sigma(g^*) = \sigma(g_m^*), \ \ m \in M \quad (48a, b)$$

and for the matrix $W_{NS}^{(r)}$, the mean and standard deviation vectors are

$$\bar{W} = \left\{\bar{W}_r\right\}, \quad r \in \vartheta; \quad \sigma(W) = \left\{\sigma\left(\bar{W}_r\right)\right\}, \quad r \in \vartheta \quad (49a, b)$$

At **step 7**, the end-member stoichiometry is selected and the quality of results is assessed. A natural criterion for selecting the "best" (optimal) end-member out of several candidates is the smallest scatter within vectors (Eqs. (47b) or (48b)). The selected mean (Eq. (47a), (48a)) gives the estimated molar Gibbs energy of the selected end member with 2σ uncertainty interval. Average value(s) of the mixing parameter(s) with 2σ uncertainty interval(s) comprise the result according to Eqs. (49a,b). An additional criterion to discard end-member candidates or mixing models is the presence of a trend over the columns in matrices (Eqs. (44)–(46)) showing inadequacy of the model (e.g., a wrong slope of the model isotherm). Results for the optimal end-member stoichiometry or non-ideal model may have some scatter, but no regular trend. It may happen that the consideration of output (Eqs. (44) (45) (46) (47a,b) (48) (49a,b)) will point that more end-member candi-

dates or yet another mixing model need to be considered. In this case, statistical DualTh calculations must be repeated beginning from Step 2, as shown on Fig. 1.

3. Results and examples

DualTh Eq. (7)–(15) used in the forward GEM thermodynamic modeling can be checked in a printout (Appendix B). For the case of AqSS equilibrium, several applications of inverse modeling DualTh methods have been published (Curti et al., 2005; Kulik and Kersten, 2002; Kulik et al., 2000). A short summary of these results is given in Section 3.1 below. A full numerical example of statistical DualTh calculations at the stoichiometric saturation is provided for the first time in Section 3.2 for the magnesium-containing calcites.

3.1. Inverse DualTh calculations for AqSS equilibria

Interaction parameters for the multi-component regular mixing model of authigenic Ca-rhodochrosite (Kulik et al., 2000) have been determined using the field characterization data for a complex natural "anoxic porewater–authigenic mineral phases" environment in organic- and sulfide-rich sediments of the Gotland Deep, Baltic Sea. A thermodynamic model of porewater chemistry at in situ $P=25$ bar and $T=5$ °C has been developed using the GEM approach. Dual chemical potentials for Mn, Ca, Fe, Mg, Sr, Ba, C, and O, calculated from the porewater composition (basis sub-system), were used in a DualTh estimation of end-member activity coefficients (Eq. (18)) in a solid solution (Mn,Ca,Mg,Sr,Ba,Fe)CO_3 taken as a non-basis sub-system. Regular interaction parameters for the composing binaries were found to be $\alpha_{Mn-Ca}=1.9\pm0.5$, $\alpha_{Mn-Mg}=0.6$, $\alpha_{Ca-Mg}=3.7$, $\alpha_{Mn-Fe}=0.2$, $\alpha_{Ca-Fe}=2.8$, $\alpha_{Mn-Sr}=9.7$, $\alpha_{Ca-Sr}=2.15$, $\alpha_{Mn-Ba}=4.0$, $\alpha_{Ca-Ba}=1.4$, all positive, but about 30% smaller than the values obtained from theoretical predictions according to Lippmann (1980). The complete equilibrium AqSS model including the (Mn,Ca,Mg,Sr,Ba,Fe)CO_3 solid solution phase was able to match the measured porewater and carbonate solid-solution compositions.

The DualTh retrieval of stoichiometry and stability of a Zn-containing end member of the Zn-doped C–S–H (calcium silicate hydrate) ternary solid solution has been done by Kulik and Kersten (2002) in extension to the previously developed ideal AqSS model for C–S–H gels at ambient conditions (Kulik and Kersten, 2001). Experimental data for five synthetic equilibrium C–S–H systems doped with 0%, 0.1%, 1%, 5%, and 10% Zn at unity (Ca+Zn)/Si molar ratio were used first to compute GEM equilibria for aqueous part of each system only, to obtain dual solution values $u_{i,q}$ for Ca, Zn, O and H. From the analysis of quasi-ternary composition diagram, six Zn-containing end-member candidates were identified: "Zn-tobermorite" $SiO_2\cdot Ca(OH)_2\cdot 0.25Zn(OH)_2\cdot H_2O$, "hardystonite" $Ca(OH)_2\cdot 0.5Zn(OH)_2$, "clinohedrite" $SiO_2\cdot Ca(OH)_2\cdot Zn(OH)_2$, "junitoite" $SiO_2\cdot 0.5Ca(OH)_2\cdot Zn(OH)_2$, "hemimorphite" $SiO_2\cdot 2Zn(OH)_2$, and the hydrated $ZnSiO_3$, with all respective solubility products unknown. Other two end-members of Zn–CSH–II ternary solid solution (non-basis sub-system) were "tobermorite" $SiO_2\cdot 0.83Ca(OH)_2\cdot 0.83H_2O$ and "jennite" $SiO_2\cdot 1.667Ca(OH)_2\cdot H_2O$. Assuming ideal ternary mixing, the statistical DualTh procedure (Eq. (41)) has been applied to find the end-member g^{o}_{298} values. The "minimum scatter" criterion pointed out at the clinohedrite and (with slightly greater σ) the hardystonite as alternative optimal Zn-containing end members.

When included into the GEM AqSS thermodynamic model of Zn–C–S–H system, both ternary solid solution models were shown to reproduce a complex sequence of reactions (leaching, carbonation) thought to occur in a long-term weathering scenario of cementitious waste forms at subsurface repository conditions. Modelling results predicted that at low to moderate Zn loading (≤1% per mole Si), Zn–C–S–H compounds can effectively immobilise Zn, but the equilibrium dissolved Zn concentrations would strongly depend on whether the clinohedrite or hardystonite Zn-containing end-member is chosen.

In a recent work (Curti et al., 2005), thermodynamics of dilute Eu-calcite solid solutions were investigated using three sets of Eu^{III} uptake experiments under widely different pH–pCO_2 conditions: (a) recrystallization in synthetic cement pore water at pH ~13 in the absence of CO_2; (b) coprecipitation in 0.1 M $NaClO_4$ at pH ~6 and pCO_2 ~1 bar; and (c) coprecipitation in synthetic seawater at pH ~8 and pCO_2 from 3×10^{-4} to 0.3 bar. At the first step, AqSS equilibria with ideal binary solid solutions between calcite and one of end-members $Eu_2(CO_3)_3$, $EuNa(CO_3)_2$, $Eu(OH)CO_3$ or $Eu(OH)_3$ with known pure-solid solubility products were computed. None of these four variants could reproduce all three experimental datasets simultaneously. At the second step, ideal binary solid solutions were constructed from calcite and one of the hypothetical Eu end-members EuO(OH), $EuH(CO_3)_2$ and $EuO(CO_3)_{0.5}$ with unknown solubility products. The statistical DualTh procedure (Eqs. (45), (48a,b)) was then used for estimating the apparent molar Gibbs energy g^{*}_{298}

(Eq. (27)) for each of seven end-member candidates. Applying both the "minimum standard deviation" and the "absence of trend" criteria for each experimental data set, it was found that no binary solid solution can describe all three sets of experimental data. Thus, the ternary solid solution models with $CaCO_3$ as a major end-member and any two of the seven possible Eu trace end-members had to be tested. All data could be modeled simultaneously only assuming an ideal solid solution $EuHCO_3$–$EuO(OH)$–$CaCO_3$, with $g^*_{EuHCO3} = -1733.0 \pm 2.3$ kJ mol^{-1} and $g^*_{EuO(OH)} = -955.0 \pm 1.8$ kJ mol^{-1}, while other end-member combinations failed. This result is thought to be consistent with the spectroscopic data for Cm^{III} and Eu^{III} indicating that two distinct species are incorporated in calcite. The study by Curti et al. (2005), essentially based on statistical DualTh results, demonstrates that heterovalent substitutions in carbonate crystal structures may need a consideration of multicomponent solid solution models.

3.2. DualTh calculations for Mg-calcite at stoichiometric saturation

This example is intended rather to illustrate some of DualTh methods described in Section 2 than to perform a sophisticated fitting of subregular interaction parameters or to review the aqueous solubility of different Mg-calcites.

Results of free-drift dissolution experiments for synthetic Mg-calcites in water (Bischoff et al., 1987) carried out at $P = 1$ bar, $T = 298$ K and $pCO_2 = 316$ Pa have been shown (Königsberger and Gamsjäger, 1992b) to plot at the equal-G curve on a Lippmann diagram, meaning that stoichiometric saturation states have been reached in these experiments. Because solubility products K_{SP} of calcite $CaCO_3$ and of possible Mg-containing end members magnesite $MgCO_3$ or dolomite $CaMg(CO_3)_2$ are, in principle, known, the data (Bischoff et al., 1987) can be used in DualTh calculations aimed at estimation of the regular Margules parameter W_G.

The basis sub-system (aqueous solution) can be GEM-modelled using the following recipe for the bulk composition of the system: 997 g H_2O + 100 kg of $C_{0.00315}N_{1.99364}O_{0.0064}$ plus certain additions of $CaCO_3$ and $MgCO_3$ such that the mole fraction of dissolved $MgCO_3$ $\chi_{Mg,aq} = m_{Mg}/(m_{Mg} + m_{Ca})$ would correspond to χ_{MgCO3} in the initial synthetic solid carbonate phase. These aqueous-gas equilibria (H_2O vapor excluded from the gas phase, $pCO_2 = 315 \pm 2$ Pa) were computed using the GEM-Selektor code to reproduce minimum stoichiometric saturation states fixed by values of pH_{ext} after kinetic extrapolation (Bischoff et al., 1987) of measured pH to the infinite time. Because, in GEM method, pH cannot be given as input variable, "inverse titration" runs were conducted, in which additions of $CaCO_3$ and $MgCO_3$ to the bulk composition b_q^{BS} were varied simultaneously while keeping χ_{Mg} constant, until the calculated equilibrium pH was equal to the reported pH_{ext} within 0.01 units. The required additions (+$CaCO_3$ and +$MgCO_3$ in millimoles) for seven selected experiments are listed in Table 1.

The source of input thermodynamic data was the Nagra-PSI data base 01/01 (Hummel et al., 2002) in GEMS-PSI version. Activity coefficients γ_j of aqueous ions of charge Z_j were calculated using the Davies equation $\log_{10}\gamma_j = -A_{DH} Z_j^2 \left(\frac{I_m^{0.5}}{1 + I_m^{0.5}} - 0.3 I_m \right)$, $I_m = \frac{1}{2}\sum_j m_j Z_j$, where I_m is effective molal ionic strength, and $A_{DH} = 0.509$ at 1 bar, 25 °C (Langmuir, 1997).

The aqueous solution was in most cases oversaturated with the calcite phase, constrained at the amount $< 10^{-9}$ mol. Typical output of GEM-solved equilibrium in the basis sub-system is given in Appendix B. The dual solutions u vectors (Eq. (34)) for all seven-basis sub-systems are collected in Table 2. To represent the synthetic Mg-calcites, five non-basis end-member stoichiometries ($CaCO_3$, $Ca_2(CO_3)_2$, $MgCO_3$, $CaMg(CO_3)_2$ and $Ca_{0.5}Mg_{0.5}CO_3$) were combined into alternative regular binary mixtures $CaCO_3$–$MgCO_3$, $Ca_2(CO_3)_2$–$CaMg(CO_3)_2$, and $CaCO_3$–$Ca_{0.5}Mg_{0.5}CO_3$. Table 3 contains basis-system chemical potentials (Eq. (40)) calculated for the five end-members, solubility products K_{SP} of which are given in Tables 4,6 and 8.

In the first statistical DualTh calculation, a regular $CaCO_3$–$MgCO_3$ (calcite–magnesite) solid solution was considered as the non-basis sub-system. Solving Eq.

Table 1
Additions of $CaCO_3$ and $MgCO_3$ to bulk compositions of basis (aqueous + gas) sub-systems for GEM equilibria calculations

Experiment #	q index	$\chi_{Mg,q}$	pH_{ext}	$CaCO_3$ added (mmol)	$MgCO_3$ added (mmol)
Calcite	0	0	7.63	1.1020	0
8B	1	0.02	7.64	1.1057	0.02256
9B	2	0.04	7.66	1.1248	0.04686
11A	3	0.08	7.68	1.1429	0.09937
17A	4	0.1	7.70	1.1776	0.13085
19A	5	0.125	7.72	1.2001	0.17144
16A	6	0.15	7.73	1.1947	0.21083

Note: Data in the χ_{Mg} and pH_{ext} columns are from Tables 1, 3, 5 in Bischoff et al. (1987).

Table 2
Calculated dual solution values for basis sub-systems (in kJ mol^{-1})

q index	$u_{Ca,q} \cdot RT$	$u_{Mg,q} \cdot RT$	$u_{C,q} \cdot RT$	$u_{Charge,q} \cdot RT$
0	−708.1547	–	−384.1225	68.9022
1	−708.0439	−618.8768	−384.1226	68.8468
2	−707.8372	−616.9002	−384.1226	68.7579
3	−707.5442	−614.7828	−384.1226	68.6205
4	−707.2464	−613.8761	−384.1226	68.4988
5	−706.9978	−613.0037	−384.1226	68.3888
6	−706.9039	−612.3855	−384.1226	68.3315

Notes: Dual solution value of oxygen is equal to $u_{O,q} \cdot RT = -12.2753$ kJ mol^{-1} in all systems; $u_{H,q} \cdot RT = -112.4532$ kJ mol^{-1} in all systems; $u_{N,q} \cdot RT = -0.004$ kJ mol^{-1} in all systems. $RT = 2.47897$ kJ mol^{-1} at $T = 298.15$ K (25 °C).

(37) is trivial in this case — the mole fractions of end members simply inherit those of Ca and Mg from Table 1. The integral molar Gibbs energy of mixture $G_{SS,q}$ is calculated using Eq. (28b), the excess Gibbs energy of mixing G_q^E — from Eq. (42), and the regular interaction parameter $W_{G,q}$ — from Eq. (43). These results are collected in Table 4, where $\alpha_q = W_{G,q}/(RT)$. It can be seen that α_q estimates somewhat increase with the mole fraction χ_2 of $MgCO_3$. Statistics for six estimated values of $W_{G,q}$ and α_q (Eq. (49a,b)) are given in Table 5. The model is strongly non-ideal and suggests a quite large miscibility gap, consistent with theoretical predictions (Urusov, 1975).

Magnesite $MgCO_3$ seems not to be the best choice to describe stability of Mg calcites because in this case, any mixing model would fail to predict the presence of two miscibility gaps and the existence of an intermediate stable phase (dolomite). Is there a better solid solution model? This can be checked by repeating the statistical DualTh calculation for the Mg end-member stoichiometries based on dolomite $CaMg(CO_3)_2$. Busenberg and Plummer (1989) selected a half disordered dolomite (hd-dolomite $Ca_{0.5}Mg_{0.5}CO_3$, $\log K_{SP} = -8.27$) as a Mg-containing end member for the crystalline "Group I" Mg-calcites, with $\log K_{SP} = -8.48$ for calcite end member. The above solubility product of hd-dolomite (Table 10 in Busenberg and Plummer, 1989) has been derived from the standard-state data of Helgeson et al. (1978, p.98–108) who interpreted the dolomite mineral reactions at 450–650 °C with account for partial disorder using the Bragg–Williams equation. The reason for selecting "disordered dolomite" most probably was that the "Group I" Mg-calcites were either natural crystalline samples or partially disordered synthetic phases prepared at 2 kbar, 700 °C or even higher pressures and temperatures (Bischoff et al., 1983, 1987).

Table 4
DualTh estimation of the Margules parameter W_G (G_{SS} and $W_{G,q}$ in kJ mol^{-1}) for the calcite–magnesite ($CaCO_3$–$MgCO_3$) solid solution at minimum stoichiometric saturation

q index	$\chi_{2,q}$	$G_{SS,q}$	$W_{G,q}$	$\alpha_q = W_{G,q}/(RT)$	$\gamma_{2,q}$	$\gamma_{1,q}$
1	0.02	−1127.21	10.82	4.365	66.17	1.002
2	0.04	−1125.15	11.67	4.709	76.69	1.008
3	0.08	−1121.07	10.92	4.403	41.54	1.029
4	0.1	−1118.86	12.60	5.083	61.40	1.052
5	0.125	−1116.20	13.03	5.258	56.00	1.086
6	0.15	−1113.67	12.27	4.949	35.72	1.118

End-member 1: $CaCO_3$; g^o_{298}(calcite) = −1129.18 kJ mol^{-1}, $\log K_{SP} = -8.48$.
End-member 2: $MgCO_3$; g^o_{298}(magnesite) = −1029.28 kJ mol^{-1}, $\log K_{SP} = -8.29$.
Values of $\log K_{SP}$ from Nagra-PSI 01/01 data base (Hummel et al., 2002).

Tables 6 and 7 contain results of DualTh calculations for the calcite–hd-dolomite solid solution variant, performed in the same way as for Tables 4 and 5. The mole fractions $\chi_{2,q}$ of hd-dolomite end-member in Table 6 are double that of the magnesite end-member in Table 4. The comparison shows that the hd-dolomite–calcite solid solution model requires a smaller interaction parameter with about two times less the uncertainty interval. Besides, the $W_{G,q}$ values in Table 6 display no significant trend; both criteria point to the hd-dolomite–calcite model as "more optimal" for these synthetic Mg calcites. This is also corroborated by a comparison of $W_G = 8.93 \pm 0.8$ kJ mol^{-1} (Table 7) with the subregular Guggenheim parameters $\alpha_0 \cdot RT = 9.86 \pm 0.2$ kJ

Table 3
Calculated basis-subsystem chemical potentials $\mu_{qm}^{(BS)}$ of end-member stoichiometries (in kJ mol^{-1})

q index	$\mu(CaCO_3)_q$	$\mu(MgCO_3)_q$	$\mu(Ca_{0.5}Mg_{0.5}CO_3)_q$	$\mu(Ca_2(CO_3)_2)_q$	$\mu(CaMg(CO_3)_2)_q$
0	−1129.103	–	–	−2258.206	–
1	−1128.992	−1039.825	−1084.409	−2257.984	−2168.818
2	−1128.786	−1037.849	−1083.317	−2257.572	−2166.634
3	−1128.493	−1035.731	−1082.112	−2256.986	−2164.224
4	−1128.195	−1034.824	−1081.510	−2256.390	−2163.020
5	−1127.946	−1033.952	−1080.949	−2255.892	−2161.898
6	−1127.852	−1033.334	−1080.593	−2255.704	−2161.186

Table 5
Statistical DualTh results for the calcite–magnesite solid solution

Parameter	W_G, kJ mol^{-1}	α_0
Average	11.89	4.79
$\pm 2\sigma$	± 1.65	± 0.67

mol^{-1} ($\alpha_0=3.98$) and $\alpha_1 \cdot RT=3.5\pm1.0$ kJ mol^{-1} regressed on a much larger set of experimental data by Busenberg and Plummer (1989), and of our $\alpha_0=3.6\pm0.3$ (Table 7) with the reported values of α_0 between 2.54 and 5.08 for Mg-calcites (Glynn, 2000).

What would happen with the DualTh results, if stoichiometries of calcite and hd-dolomite were scaled up twice together with the logK_{SP} and g^o_{298} values (to preserve the same solubility of pure end-members)? As shown in (Curti et al., 2005), such scaling would result in a different slope of the AqSS isotherm for the minor end member. Can this be detected in a statistical DualTh calculation at stoichiometric saturation? The answer is contained in Tables 8 and 9. The average interaction parameter is not much different from that in Table 7, but its standard deviation is almost three times greater. Inspection of the $W_{G,q}$ column in Table 8 shows that there is an increase of $W_{G,q}$ values with the mole fraction of dolomite. The trends are compared among all three solid solution models on Fig. 2, where it is seen that the calcite–hd-dolomite regular model is the optimal one according to the "absence of trend" criterion.

Königsberger and Gamsjäger (1992b) have measured $\log_{10}K_{SP}=-9.47$ for the crystalline (ordered?) half-dolomite, 1.2 pK units (16 times) less soluble

Table 6
DualTh estimation of the Margules parameter W_G (G_{SS} and $W_{G,q}$ in kJ mol^{-1}) for the calcite–hd-dolomite ($CaCO_3$–$Ca_{0.5}Mg_{0.5}CO_3$) solid solution

q index	$\chi_{2,q}$	$G_{SS,q}$	$W_{G,q}$	$\alpha_q=W_{G,q}/(RT)$	$\gamma_{2,q}$	$\gamma_{1,q}$
1	0.04	−1127.21	9.357	3.775	32.42	1.006
2	0.08	−1125.15	9.115	3.677	22.47	1.024
3	0.16	−1121.07	8.169	3.295	10.23	1.088
4	0.2	−1118.86	8.990	3.626	10.19	1.156
5	0.25	−1116.20	9.187	3.706	8.042	1.261
6	0.3	−1113.67	8.739	3.525	5.626	1.373

End-member 1: $CaCO_3$; g^o_{298}(calcite)=−1129.18 kJ mol^{-1}, logK_{SP}=−8.48.
End-member 2: $Ca_{0.5}Mg_{0.5}CO_3$; g^o_{298}(hd-dolomite)=−1078.59 kJ mol^{-1}, logK_{SP}=−8.27.
Values of logK_{SP} from Nagra-PSI 01/01 data base (Hummel et al., 2002); g^o_{298} for hd-dolomite is 1/2 of that for disordered dolomite (logK_{SP} also from Busenberg and Plummer, 1989).

Table 7
Statistical DualTh results for the calcite–hd-dolomite solid solution

Parameter	W_G, kJ mol^{-1}	α
Average	8.93	3.60
$\pm 2\sigma$	± 0.78	± 0.31

than the hd-dolomite considered above. How the DualTh results (Tables 6 and 7) would change if the more stable "half-dolomite" end member had been used instead of the "disordered" hd-dolomite end member?

Denoting a new standard Gibbs energy of the dolomite end-member as $g^o_2=g^o_{2,new}-\delta g^o_2$, we obtain $\delta g^o_2=-1.2\cdot RT\ln 10=-6.85$ kJ mol^{-1}. Substitution into Eq. (43) and re-arrangement leads to $W_{G,q,new}=W_{G,q,old}+\delta W_{G,q}$ where $\delta W_{G,q}=\dfrac{-\delta g^o_2}{\chi_{q,1}}$ because other terms in Eq. (43) remain the same. The difference $\delta W_{G,q}$ between the new and the old estimate of the Margules parameter should increase with the mole fraction of the half-dolomite end member. Table 10 contains new α_q values obtained with the above two equations from "old" values of Table 6. It is seen that $W_{G,q}$ values for $q=4$, 5 and 6 are 1 to 2 kJ mol^{-1} above those for $q=1$, 2 and 3, i.e., show some trend. The $W_{G,q}$ or α_q averages have more than twice larger 2σ uncertainty intervals than in Table 7 for the hd-dolomite end-member. Thus, both statistical DualTh criteria tell that half-dolomite ($\log_{10}K_{SP}=-9.47$) is a less favorable choice of the Mg-containing end member than hd-dolomite ($\log_{10}K_{SP}=-8.27$) for modelling this set of stoichiometric saturation data.

Königsberger and Gamsjäger (1992b) re-interpreted stabilities of Mg-calcites in terms of the "dilute solid solution formalism" (Bale and Pelton, 1990), considering a binary solid solution made of a "solvent" A

Table 8
DualTh estimation of the Margules parameter W_G (G_{SS} and $W_{G,q}$ in kJ mol^{-1}) for the calcite–d-dolomite ($Ca_2(CO_3)_2$–$CaMg(CO_3)_2$) solid solution

q index	$\chi_{2,q}$	$G_{SS,q}$	$W_{G,q}$	$\alpha_q=W_{G,q}/(RT)$	$\gamma_{2,q}$	$\gamma_{1,q}$
1	0.04	−2254.42	7.873	3.176	18.67	1.005
2	0.08	−2250.30	8.841	3.566	20.46	1.023
3	0.16	−2242.14	8.229	3.320	10.40	1.089
4	0.2	−2237.72	10.23	4.125	14.02	1.179
5	0.25	−2232.39	10.94	4.413	11.97	1.318
6	0.3	−2227.35	10.27	4.142	7.610	1.452

End-member 1: $CaCO_3$; g^o_{298}(2calcite)=−2258.35 kJ mol^{-1}, logK_{SP}=−16.96.
End-member 2: $CaMg(CO_3)_2$; g^o_{298}(d-dolomite)=−2157.15 kJ mol^{-1}, logK_{SP}=−16.54.
logK_{SP} of dolomite from Nagra-PSI 01/01 data base (Hummel et al., 2002); g^o_{298} for "2calcite" is twice that of calcite.

Table 9
Statistical DualTh results for the 2 calcite–d-dolomite solid solution

Parameter	W_G, kJ mol^{-1}	α
Average	9.40	3.79
$\pm 2\sigma$	± 2.28	± 0.92

(calcite) and a "solute" B (e.g., magnesite) end members. The molar Gibbs energy of this solution is

$$G_{SS} = (1-\chi)g_A^o + \chi g_B^o + RT[(1-\chi)\ln(1-\chi) + \chi\ln\chi] + RT\left[\chi\ln\gamma_B^\infty + \frac{\varepsilon'}{2}\chi^2 + \frac{\varepsilon''}{2}\chi^3 + \ldots\right] \quad (50)$$

where χ is the mole fraction of the solute; γ_B^∞ is the activity coefficient of the solute at infinite dilution $\chi \to 0$; ε',ε'',...are the ...first-, second-, ...order interaction coefficients. The last term in Eq. (50) is the excess Gibbs energy of mixing G^E. The activity coefficients are:

$$\ln\gamma_A = -\frac{\varepsilon'}{2}\chi^2 - \frac{\varepsilon''}{2}\chi^3 - \ldots \quad (51)$$

$$\ln\gamma_B = \ln\gamma_B^\infty + \ln\gamma_A + \varepsilon'\chi + \varepsilon''\chi^2 + \ldots \quad (52)$$

When only the first-order parameter ε' is retained ($\varepsilon'' = \ldots = 0$), the relationship $\ln\gamma_B^\infty = -\varepsilon'/2$ reduces the "dilute formalism" to the regular mixing model (Königsberger and Gamsjäger, 1992b) with $\alpha_0 = -\varepsilon'/2$. These authors, using the solutus (equilibrium) co-pre-

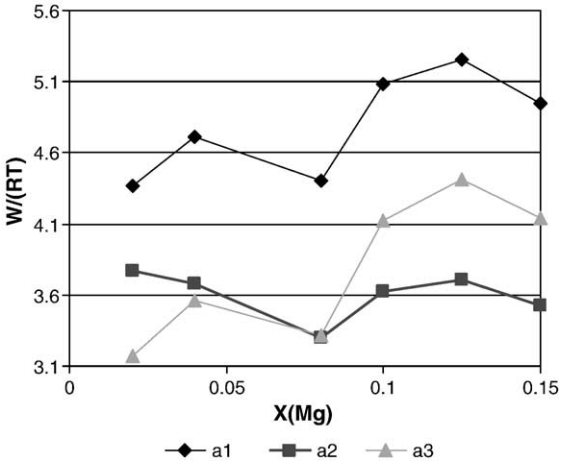

Fig. 2. Comparison of trends in DualTh-estimated values of regular Margules parameter $\alpha_0 = W/(RT)$ versus mole fraction of Mg (X(Mg)) for three alternative solid solution models: a1 — Table 4; a2 — Table 6; a3 — Table 8. The a2 model (calcite–hd-dolomite) seems to produce α_q values independent of X(Mg) and having the smallest scatter. Lines are just guides for the eye and do not represent any regressions or model fits.

Table 10
Estimated parameter W_G (in kJ mol^{-1}) for the calcite–half-dolomite ($CaCO_3$–$Ca_{0.5}Mg_{0.5}CO_3$) solid solution

q index	$W_{G,q}$	$\alpha_q = W_{G,q}/(RT)$
1	16.492	6.653
2	16.561	6.680
3	16.324	6.585
4	17.553	7.080
5	18.320	7.390
6	18.525	7.473

Using $\log K_{SP} = -9.47$ (Königsberger and Gamsjäger, 1992a) of the half-dolomite end member and "old" $W_{G,q}$ values from Table 6 (see text for explanations). Averages (with 2σ uncertainty): $W_G = 17.30 \pm 1.78$ kJ mol^{-1}; $\alpha = 6.98 \pm 0.72$.

cipitation data (Mucci and Morse, 1984), have estimated for the solution of magnesite in calcite $\ln\gamma_B^\infty = 4.96 \pm 0.2$. This compares (fortuitously?) well with our result ($\alpha_0 = 4.79 \pm 0.67$, Table 5) obtained from a different set of experimental data. However, their ε' parameter estimate ($\varepsilon' = 3.69 \pm 1.79$) is inconsistent with $\ln\gamma_B^\infty = 4.96$ that would lead to $\varepsilon' \approx -10$ in the case of regular mixing.

Is our "optimal" regular model with hd-dolomite end member B (Tables 6 and 7) consistent with the "dilute formalism" truncated to the first interaction parameter? To check this, the excess Gibbs energy of mixing has been calculated using the modified DualTh Eq. (42): $G_q^E = G_{SS,q}^{(BS)} - RT\left[\chi_q\ln\chi_q + (1-\chi_q)\ln(1-\chi_q)\right] - \left[\chi_q g_B^o + (1-\chi_q)g_A^o\right]$. Parameter ε' values were found from the equation $\varepsilon_q' = \frac{2}{\chi_q^2}\left(\frac{G_q^E}{RT} - \chi_q\ln\gamma_B^\infty\right)$ taking $\ln\gamma_B^\infty = \alpha_o = 3.6$ (Table 7). Results are presented in Table 11. The ε'_q outlier at $q = 1$ points that the estimation of solute–solvent interaction parameter ε' may be very sensitive to the experimental errors in solid solute mole fraction χ_q. Hence, the average and standard deviation were also computed over 5 remaining points (with-

Table 11
Estimated parameter ε' for the dilute solid solution of hd-dolomite $Ca_{0.5}Mg_{0.5}CO_3$ (solute B) in calcite (solvent A)

q index	$\chi_{B,q}$	$G_{SS,q}$	G_q^E	ε'_q
1	0.04	−1127.21	0.3627	2.9032
2	0.08	−1125.15	0.6739	−5.0528
3	0.16	−1121.07	1.1055	−10.159
4	0.2	−1118.86	1.4425	−6.9057
5	0.25	−1116.20	1.7265	−6.5132
6	0.3	−1113.67	1.8473	−7.4402

Values of $G_{SS,q}$ and G_q^E in kJ mol^{-1}.
Using $\log K_{SP} = -8.27$ (Table 6) of the hd-dolomite end member (see text for explanations). Average of ε' (with 2σ uncertainty): -5.53 ± 8.91. Average without the outlying value of ε'_q at $q = 1$: $\varepsilon' = -7.214 \pm 3.74$.

out $q=1$). Thus obtained value of $\varepsilon' = -7.21 \pm 3.74$, although rather uncertain, is consistent with the theoretical requirement $\ln\gamma_B^{\infty} = -\varepsilon'/2$ for the regular mixing. This result corroborates our earlier conclusion about the hd-dolomite with $\log_{10}K_{SP} = -8.27$ as the optimal end-member for the regular model description of synthetic Mg-calcites. Note that all attempts to repeat estimation of ε' using a different solubility product of hd-dolomite or another Mg end-member (magnesite, full dolomite) resulted in inconsistent α_0 and ε' values or in a very large scatter of ε'_q (not shown). The DualTh methods and criteria seem to be useful also if applied with the dilute solid solution formalism.

4. Discussion

4.1. Comparison of DualTh with earlier methods

The GEM DualTh technique is just one of existing methods for estimating thermodynamic properties of solid solution end members or mixing parameters using experimental data for the co-existing aqueous phase. Below, some earlier methods are outlined for comparison.

4.1.1. The "*activity ratios*" technique

McCoy and Wallace (1956) evaluated free energies of mixing in KCl–KBr solid solutions at 25 °C from known solubilities of the pure salts and the solid solutions in water and measured activity coefficients in the saturated aqueous ternary systems. The chemical potential difference of KCl (component 1) in solid solution and in pure solid is $(\mu_1 - \mu_1^o) = RT(\ln a_1'' - \ln a_1')$, where a_1'' is the activity of KCl in the saturated aqueous phase, and a_1' is the activity of KCl in the aqueous phase saturated with pure KCl at the same temperature. In the same manner for KBr (component 2), $(\mu_2 - \mu_2^o) = RT(\ln a_2'' - \ln a_2')$. The molar Gibbs energy of mixing in the solid solution, $G_{SS}^{(mix)} = G_{SS} - G_{SS}^o$, now becomes (see also Eqs. 1 and 7 in (Christov, 1996)):

$$G_{SS}^{(mix)} = RT(\chi_1 \ln a_1 + \chi_2 \ln a_2) = G_{SS} - (\chi_1 g_1^o + \chi_2 g_2^o) \tag{53}$$

or

$$G_{SS}^{(mix)} = \chi_1(\mu_1 - \mu_1^o) + \chi_2(\mu_2 - \mu_2^o) = RT[\chi_1(\ln a_1'' - \ln a_1') + \chi_2(\ln a_2'' - \ln a_2')] \tag{54}$$

By combining Eqs. (53) and (54), it is possible to eliminate G_{SS}^{mix} and to find either g_j^o of a solid solution end member, or G^E and interaction parameter(s), if mole fractions of end-members in solid solution χ_j, dissolved molalities m_j, and mean aqueous activity coefficients $\gamma_j^{(aq)}$ of the components are known. The values of m_j can be measured; the values of $\gamma_j^{(aq)}$ can also be measured with isopiestic techniques, or calculated using individual ion activity coefficients obtained from the Debye–Hückel, SIT, or Pitzer equations, depending on the ionic strength. For highly soluble salt-water systems, the Pitzer equations have routinely been used (Christov et al., 1994; Filippov and Rumyantsev, 1990; Harvie et al., 1984). Results of inverse calculations using Eq. (54) will depend on the applicability of the electrolyte model of choice to the system of interest. For instance, the Debye–Hückel ion association models (cf.(Langmuir, 1997; Morel and Hering, 1993)) can be used with reasonable accuracy up to 0.1–0.5 *m* effective ionic strengths. The SIT model (Grenthe et al., 1997) can be used up to 3 *m* ionic strength. The Pitzer model is applicable to mixed electrolytes of any ionic strength with accuracy of 2% to 6% (Pitzer and Kim, 1974). Of course, the same limitations related to the account for aqueous non-ideality apply also to GEM DualTh calculations.

What are then the advantages of the inverse modeling DualTh methods over the estimation of $G_{SS}^{(mix)}$ from equations like (54)? Firstly, it is the simplicity of DualTh determination of equilibrium chemical potential of a solid solution end member using Eq. (16), which does not involve molalities or aqueous activity coefficients directly. Secondly, in Eq. (54), the mean activity coefficients are used, whereas in most computer speciation codes, individual ionic species and complexes are considered with the respective activity coefficients. Thirdly, DualTh equations do not depend on the complexity of the basis sub-system; the only requirement is that the underlying thermodynamic model is adequate for the system of interest. The parameterized non-basis sub-system can be included later into the GEM forward model for checking or sensitivity studies, if necessary.

4.1.2. Lippmann diagrams and MBSSAS code

In aquatic geochemistry, the Lippmann phase diagram and total solubility product (Lippmann, 1977, 1980, 1982) became a popular tool for analyzing pseudo-binary AqSS equilibria after publications by Glynn (Glynn and Reardon, 1990; Glynn et al., 1990; Glynn, 2000) enhanced with the MBSSAS code for calculating and plotting such diagrams and retrieval of Margules parameters and equilibrium relations (Glynn, 1991). The Lippmann concept has been extended and deep-

ened in the framework of the "unified theory of solid solution solubility" by Gamsjäger and Königsberger (Gamsjäger et al., 2000; Königsberger and Gamsjäger, 1992a), as well as Prieto et al. (2000) and many others.

The equilibrium between the aqueous electrolyte and the mixed ionic solid $(B, C)A$ is expressed by two law-of-mass action equations:

$$[B^+][A^-] = K_{BA} a_{BA} = K_{BA} \chi_{BA} \gamma_{BA} \tag{55a}$$

$$[C^+][A^-] = K_{CA} a_{CA} = K_{CA} \chi_{CA} \gamma_{CA} \tag{55b}$$

where $[A^-]$, $[B^+]$, $[C^+]$ are the aqueous activities of A^-, B^+, C^+ (or A^{2-}, B^{2+}, C^{2+}); K_{BA} and K_{CA} are the solubility products of pure BA and CA end-members with activities a_{BA}, a_{CA}, mole fractions χ_{BA}, χ_{CA}, and activity coefficients γ_{BA}, γ_{CA}, respectively. Using the Lippmann total solubility product, $\Sigma\Pi = [A^-]([B^+]+[C^+])$, the equilibrium $\Sigma\Pi$ value can be expressed as

$$\Sigma\Pi_{eq} = K_{BA} \chi_{BA} \gamma_{BA} + K_{CA} \chi_{CA} \gamma_{CA} \tag{56}$$

defining the solidus curve. The Lippmann solutus curve equation is (e.g., (Glynn, 1991)):

$$\Sigma\Pi_{eq} = \frac{1}{\left(\frac{\chi_{B,aq}}{K_{BA}\gamma_{BA}} + \frac{\chi_{C,aq}}{K_{CA}\gamma_{CA}}\right)} \tag{57}$$

where the aqueous activity fractions of B and C are defined as

$$\chi_{B,aq} = \frac{[B^+]}{[B^+]+[C^+]}; \quad \chi_{C,aq} = \frac{[C^+]}{[B^+]+[C^+]}. \tag{58a, b}$$

The solidus and solutus curves drawn on a Lipmann diagram with the common ordinate $\Sigma\Pi_{eq}$ and two superimposed abscissas χ_{CA} and $\chi_{C,aq}$ (note that $\chi_{BA}=1-\chi_{CA}$ and $\chi_{B,aq}=1-\chi_{C,aq}$) define a series of possible equilibrium states for a pseudo-binary AqSS system. It is inherently assumed that activity–concentration relations in the aqueous phase are set by the appropriate aqueous speciation model, just as in other methods described above. Other useful curves drawn on Lippmann diagrams include (Glynn, 1991): the minimum stoichiometric saturation curve for the solid $B_{1-x}C_xA$

$$\Sigma\Pi_{mss} = \frac{K_{CA}^x K_{BA}^{1-x} a_{CA}^x a_{BA}^{1-x}}{\chi_{BA}^{1-x} \chi_{CA}^x} \tag{59}$$

where $\chi_{BA}=\chi_{B,Aq}$ (this curve can be drawn for the entire solid-solution range regardless of the miscibility gap); and the distribution coefficient defined as

$$D = \frac{\chi_{BA}/\chi_{CA}}{[B^+]/[C^+]} = \frac{K_{CA}\gamma_{CA}}{K_{BA}\gamma_{BA}} \tag{60}$$

which depends on the composition of the solid in the case of non-ideal mixing. For instance, in the regular binary Margules model, Eq. (60) takes the form $D = \frac{K_{CA}\exp(\alpha\chi_{BA}^2)}{K_{BA}\exp(\alpha\chi_{CA}^2)}$

By equating Eqs. (56) and (57) and using Eq. (60), one obtains

$$(1-D)(1-\chi_{C,aq})\chi_{CA} + \left(1-\frac{1}{D}\right)(1-\chi_{CA})\chi_{C,aq} = 0 \tag{61}$$

By solving it algebraically, the solid mole fraction χ_{CA} is found from aqueous fraction $\chi_{C,aq}$

$$\chi_{CA} = \left(1 + D\frac{1-\chi_{C,aq}}{\chi_{C,aq}}\right)^{-1} \tag{62}$$

Finding χ_{CA} from known $\chi_{C,aq}$ at equilibrium may be more useful:

$$\chi_{C,aq} = \left(1 + \frac{1-\chi_{CA}}{D\cdot\chi_{CA}}\right)^{-1}. \tag{63}$$

If $\chi_{C,aq}$ and χ_{CA} are known from equilibrium experiments then solving Eq. (62) for D yields

$$D = \frac{(\chi_{CA}-1)\chi_{C,aq}}{\chi_{CA}(\chi_{C,aq}-1)}. \tag{64}$$

Then, using Eq. (60), either the activity coefficient or the solubility product of the solid solution end member can be found. In the case of regular mixing, the interaction parameter W_G can be retrieved even from a single experiment:

$$W_G = \frac{RT(\ln D + \ln K_{BA} - \ln K_{CA})}{(1-\chi_{CA})^2 - \chi_{CA}^2}. \tag{65}$$

Lippmann diagrams also help determining the binodal and spinodal miscibility gaps, and finding the critical, peritectic, eutectic and alyotropic points (Glynn, 1991, 2000). An example Lippmann diagram for the calcite–hd-dolomite AqSS system (already parameterized using DualTh calculations in Section 3.2) is shown on Fig. 3.

The main limitation of Lippmann functions and diagrams seems to lie in the fact that they were developed for the aquatic pseudo-binary ionic systems such as (B,C)A or C(A,B), and become intractable for ternary or higher-order systems, or for complex solids. Alike the "activity ratio" method (Eq. (54)), Lippmann functions use ionic activities and activity fractions and, thus, depend on the choice of aqueous speciation and activity coefficient model. Note that any quantity defined in Eqs. (57)–(65) can be

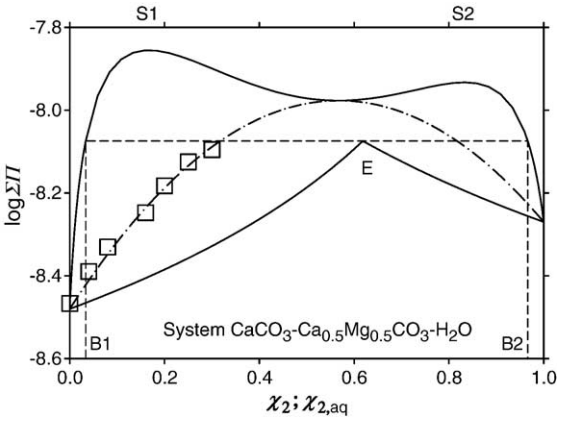

Fig. 3. Lippmann diagram of the $CaCO_3$–$Ca_{0.5}Mg_{0.5}CO_3$ binary AqSS system, constructed using the MBSSAS code (Glynn, 1991) from $\log K_{BA} = -8.27$ (hd-dolomite, end-member 2 or B), $\log K_{CA} = -8.48$ (calcite, end-member 1 or C), see Table 6, and $\alpha_0 = 3.6$ (see Table 7), $\alpha_1 = 0$. The solidus is the uppermost curve; the solutus is the lowermost curve with a eutectic point E; and the equal-G (minimum stoichiometric saturation) curve is dot-dashed. The dashed horizontal line through the E point at $\log \Sigma\Pi = -8.0745$ crosses the solidus at two binodal compositions B1 and B2 defining a miscibility gap at $0.034 < \chi_2 < 0.966$. Two maxima on the solidus curve point to the spinodal compositions S1 at $\chi_2 = 0.167$ and S2 at $\chi_2 = 0.833$. Squares show selected experimental points (Bischoff et al., 1987) also used in the GEM DualTh calculations (Table 1). The $\Sigma\Pi_q$ values for experimental points were calculated from the equation $\Sigma\Pi_q = a\left(CO_3^{2-}\right)_q \cdot \left[a\left(Ca^{2+}\right)_q + a\left(Ca^{2+}\right)_q^{0.5} \cdot a\left(Mg^{2+}\right)_q^{0.5}\right]$ (Eq. (50) in Glynn, 1991) where $a()_q$ denote aqueous activities taken from GEM calculations of equilibria in q-th basis sub-system. These $\Sigma\Pi_q$ values were then plotted against solid mole fractions of hd-dolomite $\chi_{2,q}$ from Table 6.

computed in forward GEM calculations of AqSS equilibria. For instance, Lippmann diagrams can be plotted from a series of GEM-calculated activities and mole fractions at varying bulk composition of the AqSS system.

4.1.3. Weighted least-squares and Bayesian estimation techniques

Least-squares regression methods (e.g., (Box et al., 1978)) can yield robust statistical estimates of e.g., interaction parameters, if many AqSS experimental points at different compositions are available. In general, such methods minimize the (scalar) error function

$$E(p) = [f(p) - y]^{\mathrm{T}} C_y^{-1} [f(p) - y] \quad (66)$$

where y is a vector of experimental data (e.g., $n(Q)$ distribution coefficients), p is a vector of $n(M)$ adjustable parameters (e.g., Margules parameters), and C_y is the covariance matrix of the experimental data vector. The inverse C_y^{-1} of C_y equals the weighting matrix.

Königsberger (1991) has suggested an improved "Bayesian least squares" technique of thermodynamic parameter estimation, also implemented as a subroutine in the ChemSage modeling code (Königsberger and Eriksson, 1995). In this technique, the objective function $E(p)$ consists of two parts: (1) the difference between predicted and experimental data (Eq. (66)), and (2) the difference between estimated (p) and a priori parameter values (p^{o}):

$$E(p) = [f(p) - y]^{\mathrm{T}} C_y^{-1} [f(p) - y] + [p - p^{\mathrm{o}}]^{\mathrm{T}} C_{p^{\mathrm{o}}}^{-1} \times [p - p^{\mathrm{o}}] \quad (67)$$

where $C_{p^{\mathrm{o}}}^{-1}$ equals the weighting matrix for the a priori parameters vector. In this way, it is possible to weight the two parts of the deviation function $E(p)$ differently, depending on whether more confidence is put on the experimental data or on the inherent model properties that can be independently estimated or predicted.

Due to the progress in atomistic modeling of mixing in solid solution structures (Becker et al., 2000; Becker and Pollok, 2002), more predicted parameters, in principle, can be collected in the a priori vector p^{o} (Eq. (67)). This indicates a potential importance of the Bayesian estimation approach, which can also be applied to the results of DualTh retrieval of solid solution parameters, thus enhancing the quality of "statistical" DualTh techniques. However, the effect of advanced statistic or regression methods applied to the data on (sparingly soluble) AqSS systems is quite often marred by the scarcity of experimental points at different solid compositions, kinetic problems in attaining equilibrium at low temperatures, and large experimental errors in measured compositions of co-existing aqueous and solid solution phases.

4.2. Is the aquatic basis sub-system the only possible one?

In this contribution, only AqSS systems have been considered. In such systems, the dual chemical potentials u_i are extracted from the GEM-modeled equilibrium in the basis sub-system that includes the aqueous electrolyte. In general, other basis sub-systems containing either the gas mixture or the mixed fluid phase, but no aqueous electrolyte, can also be considered (I.K.Karpov, personal communication). In such cases, the non-basis sub-system may include

solid (or liquid) solution end members, components of the silicate melt, etc. The bulk composition of the gas phase (e.g., volcanic gas) can be sampled in the field and measured; the composition of the fluid can be estimated e.g., from studies of fluid inclusions in rock-forming minerals; and that of the solid solution or volcanic glass can be measured using the (microprobe) X-ray techniques. As in the case of AqSS systems, the ultimate requirements are that the basis sub-system composition must be representative for all chemical elements that comprise the non-basis sub-system, and the thermodynamic model of non-ideal fluid or gas mixture must be adequate. The latter requirement appears difficult to meet, especially for near- and supercritical hydrothermal aqueous fluids.

5. Conclusions

1. Dual-thermodynamic (*DualTh*) calculations simplify both forward and inverse thermodynamic modelling of heterogeneous systems involving several variable-composition phases, such as AqSS (aqueous–solid solution) systems. The DualTh approach exploits the ability of Gibbs energy minimisation (GEM) algorithms to find simultaneously two numerical solutions (*primal* and *dual*) of the isobaric–isothermal (geo)-chemical equilibrium speciation problem. DualTh methods compare primal and dual values of chemical potential for a given chemical species and also between the components of equal stoichiometry in the co-existing phases.

2. In the forward GEM modelling of the equilibrium speciation and element partition between solid solutions, gas, and aqueous electrolyte phases, the DualTh relations resulting from the Karpov–Kuhn–Tucker conditions of chemical equilibrium, are used in a simple and straightforward retrieval of activities and their functions such as pH and Eh directly from the species stoichiometry and the dual solution chemical potentials.

3. Application of DualTh methods in the inverse modelling requires to subdivide the chemical thermodynamic system of interest into: (i) *basis sub-system* (containing a multi-component phase such as aqueous electrolyte with known thermodynamic data and mixing properties for all species), in which the dual chemical potentials are found by computing equilibrium states using the GEM algorithm; and (ii) *non-basis* sub-system containing species or phases with some unknown input parameters, to which dual chemical potentials are applied later on.

4. The DualTh approach is shown to provide a useful alternative to other existing methods (e.g., Lippmann diagrams, "activity ratios"): (i) in finding (apparent) standard chemical potentials of (trace) solid-solution end-members; (ii) in estimating activity coefficients and mixing parameters using known experimental bulk compositions of co-existing aqueous and solid-solution phases. These tasks can be performed when the solid solution is experimentally shown to co-exist with the aqueous phase either at the equilibrium or at the minimum stoichiometric saturation state.

5. When multiple AqSS partitioning experiments are available, the GEM inverse modelling results can be much improved by using the statistical DualTh calculations that allow the selection of an "optimal" end-member stoichiometry out of several alternative candidates. As demonstrated in example calculations for Mg-calcites, the parameters of interest are then found with both mean values and uncertainty intervals. This procedure can be further enhanced by the application of Bayesian weighted least-squares regression methods.

6. The main motivation for using GEM DualTh techniques consists in the simplicity of DualTh determination of equilibrium chemical potential of a solid solution end member, without involving molalities or aqueous activity coefficients explicitly. DualTh equations do not depend on the complexity of the basis subsystem; the only requirement is that the underlying thermodynamic model is adequate for the system of interest. The (parameterized) non-basis sub-system can be included later into the GEM forward model for checking or sensitivity studies, although this is generally not necessary.

Acknowledgments

The author is indebted to I.K. Karpov and M.Kersten for many years of exchange of ideas that have led to implementation of DualTh concepts in the GEM-Selektor code and their application to various AqSS systems. Fruitful discussions with E. Curti, U. Berner, J. Tits, W. Hummel at the PSI, and with D. Bosbach, J. Bruno, Th. Fanghanel, H. Gamsjäger, P. Glynn, E. Königsberger, V. Kurepin, L. Lakshtanov, M. Prieto, Th. Wagner, and others are greatly appreciated. Thoughtful reviews by H. Gamsjäger and E. Königsberger helped much in improving the quality of the revised paper. This work has been financially supported in part by the National Cooperative for the disposal of radioactive waste (Nagra), Wettingen, Switzerland. **[LW]**

Appendix A

For a pure substance phase, any equation like (Eq. (15)) yields the numerical value of its saturation index SI. To prove this statement, compare the definition of SI with the definition of the reaction quotient $Q_r = a_{M+}a_{L-}$ for the ML ionic solid (reaction $ML = M^+ + L^-$ with equilibrium constant K_S assuming the unity activity of the solid):

$$10^{\Omega_S} = Q_r/K_S = (a_{M+}a_{L-})/K_S. \qquad (A1-1)$$

Regardless of presence of the solid in the system, activities of aqueous ions M^+ and L^- can be found using Eq. (9), and, in turn, the reaction quotient can be calculated as

$$\ln Q_r = \left[u_M + u_{Charge} - g^o_{M+}/RT\right] + \left[u_L - u_{Charge} - g^o_{L-}/RT\right] = u_M + u_L - \left(g^o_{M+} + g^o_{L-}\right)/(RT).$$

The solubility product K_S can be found as $-RT\ln K_S = (g^o_{M+} + g^o_{L-}) - g^o_{ML}$. By substituting it and the above equation into Eq. (A1-1), one obtains

$$\Omega_S = \frac{1}{\ln 10}\ln(Q_r/K_S)) = \frac{1}{\ln 10}\left(u_M + u_L - g^o_{ML}/RT\right), \qquad (A1-2)$$

the rightmost part of which has ***exactly*** the same form as Eq. (15). This gives the proof which can be repeated for any pure solid dissolution reaction.

Appendix B

Example printout of GEM-calculated basis-system equilibrium state (q=4, experiment #17A).

GEM-Selektor v.2-PSI: Calculation of equilibrium state in the system: DualTh:G:MgCalcBMB:1050:0:1:25:000: 14/12/2004 09:49.

Basis sub-system for Mg-calcite (Bischoff et al., 1987), exp. 17A.

State variables: P(bar)=1 T = 25 (C) = 298.15 (K) V(cm^3) = 88333779 Mass(kg) = 100.9971313 Min.potential (moles): G($\boldsymbol{x}$) = −7159.06733.

Table A2-1
Parameters of independent components (IC, stoichiometry units)

IC name	Input bulk composition, moles	Residual of mass balance	IC chemical potential	
			mol/mol	J/mol
ICnam	b	δb	u	$u \cdot RT$
C	11.22543476	−2.35e−12	−154.9524	−384122.6
Ca	0.00117762	2.909e−13	−285.2983	−707246.4
H	110.6836991	−2.117e−12	−45.36284	−112453.2
Mg	0.000130847	1.938e−13	−247.6334	−613876.1
Nit	7103.767147	1.819e−12	−0.0016024	−4.0
O	78.15034841	−6.726e−12	−4.951755	−12275.3
Zz	0	9.432e−16	27.63197	68498.8

Aqueous phase: I (molal)=0.003855 pH=7.7 pe=12 Eh(V)=0.7085.

Table A2-1A
Total dissolved independent components

IC name	Molality (mol/kg H_2O)	log(molality)	log(molarity)	Concentration (g/kg-soln)
ICnam	m_{Tot}	$\log_{10} m_{Tot}$	$\log_{10} M_{Tot}$	C_{Tot}
C	0.002715394	−2.56617	−2.56747	0.03260648
Ca	0.00118119	−2.92768	−2.92899	0.04732873
H	0.002592608	−2.58626	−2.58757	0.002612612
Mg	0.0001312438	−3.88192	−3.88323	0.003189139
Nit	0.00129373	−2.88816	−2.88946	0.01811668
O	0.008039658	−2.09476	−2.09607	0.1285998
Zz	−9.46184e−16	0	0	−0

Table A2-2
Parameters of dependent components (DC, species)

Species name	Type	Quantity in the system	Concentration	Activity coeff.	Log activity	Chemical potential
DCnam	DCC	x_j (mol)	m_j	γ_j	$\log_{10} a_j$	μ_j (J/mol)
$Ca(CO_3)@$	S	8.22493e-06	8.2499e-06	1	−5.084	−1128195
$Ca(HCO_3)^+$	S	2.84424e-05	2.8529e-05	0.9347	−4.574	−1172149
Ca^{+2}	S	0.00114094	0.0011444	0.7635	−3.059	−570249
$CaOH^+$	S	7.7591e-09	7.7826e-09	0.9347	−8.138	−763476
$Mg(CO_3)@$	S	5.25726e-07	5.2732e-07	1	−6.281	−1034824
$Mg(HCO_3)^+$	S	2.9324e-06	2.9413e-06	0.9347	−5.564	−1078779
Mg^{+2}	S	0.00012737	0.00012776	0.7635	−4.011	−476878
$MgOH^+$	S	1.90951e-08	1.9153e-08	0.9347	−7.75	−670106
$CO_2@$	S	0.000106896	0.00010722	1	−3.97	−408673
CO_3^{-2}	S	7.35176e-06	7.3741e-06	0.7635	−5.249	−557946
HCO_3^-	S	0.00255281	0.0025606	0.9347	−2.621	−601900
$CH_4@$	S	0	0	1	−140.1	−833935
$H_2@$	S	0	0	1	−42.51	−224906
$N_2@$	S	0.000644909	0.00064687	1	−3.189	−8
$O_2@$	S	6.55102e-08	6.5709e-08	1	−7.182	−24551
OH^-	S	5.3531e-07	5.3693e-07	0.9347	−6.299	−193227
H^+	T	2.12437e-08	2.1308e-08	0.9347	−7.7	−43954
$H_2O@$	W	55.3406	0.99992	1	−3.627e-05	−237182
CO_2	G	11.2227	0.0031495	1	−2.502	−408673
CH_4	G	0	0	1	−137.2	−833935
H_2	G	0	0	1	−39.4	−224906
N_2	G	3551.88	0.9968	1	−0.001392	−8
O_2	G	0.17816	4.9999e-05	1	−4.301	−24551
Gr	O	0	1	1	−67.29	−384123
Cal	O	1e-09	1	1	0.1719	−1128195
Portlandite	O	0	1	1	−10.46	−956703
Mgs	O	0	1	1	−0.9722	−1034824
Brc	O	0	1	1	−5.449	−863333

Concentration and activity are given for aqueous species in mol/(kg H_2O), for other species–in the mole fraction scale. For single-component minerals, $\log_{10} a_j$ equals the saturation index SI.

Table A2-3
Parameters of phases at equilibrium state

Phase name	Type	N. of spec.	Quantity in the system	Phase mass	Phase volume	Stability criterion
PHnam	PHC	L1	Xa (moles)	phM (g)	phVol (cm3)	Fa
aq_gen	a	18	55.3452	997.21	999.98	−2.411e−09
gas_gen	g	5	3563.28	1e+05	8.8333e+07	3.326e−11
Graphite Gr	s	1	0	0	0	0
Calcite Cal	s	1	1e−09	1.001e−07	3.6934e−08	0.4856
Portlandite	s	1	0	0	0	0
Magnesite Mgs	s	1	0	0	0	0
Brucite Brc	s	1	0	0	0	0

Use the L1 column (number of species per phase) to locate the species in Table A2-2. Note that calcite amount was constrained from above at 10^{-9} mol.

Appendix C. Main symbols and abbreviations

Symbol	Explanation	Symbol	Explanation
A	Stoichiometry matrix	M	Matrix and a set used in Eq. (40)
a	Activity (of a component)	m	Molal concentration (mol kg^{-1})
AqSS	Aqueous-solid solution (system)	μ^o	Standard chemical potential
α	Redlich–Kister interaction parameter	μ	Primal chemical potential
B	Matrices defined in Eqs. (32),(33)	N	Set of stoichiometry units
b	Bulk composition vector	$n(N)$	Number of elements in the set N
$^{(BS)}$	Basis sub-system superscript	$^{(NS)}$	Non-basis sub-system superscript
C	Concentration (of a component)	Ω_S	Saturation index (Eq. (14))
C_y	Covariance matrix (Eqs. (66), (67))	P	Pressure (bar)
D	Distribution coefficient (Eq. (60))	Q_r	Reaction quotient
$\Delta_r G^o$	Standard Gibbs energy of reaction	Q	Set of experimental compositions
E_p	Objective function (Eqs. (66), (67))	q	Index of experiment
ε', ε'',...	"Dilute formalism" parameters	R	Universal gas constant, 8.3145 J K^{-1} mol^{-1}
F	Faraday constant, 96485 C mol^{-1}	r	Relative content (Eq. (8))
f^o, f	(Standard) fugacity (of a gas)	$\Sigma\Pi$	Lippmann total solubility product
$G(x)$	Total Gibbs energy function	SI	Saturation index of a pure phase (Ω_S)
G^o	Matrix defined in Eq. (44)	σ	Standard deviation
G^*	Matrix defined in Eq. (45)	T	Temperature (K), °C if indicated
G^E	Excess Gibbs energy (of mixing)	^{T}	Transpose operator
G_{SS}	Integral Gibbs energy of mixture	U	Matrix defined in Eq. (34)
g^o	Standard Gibbs energy function	u	Dual solution (vector)
g^*	Apparent Gibbs energy (Eq. (27))	υ	Normalized primal chemical potential
GEM	Gibbs energy minimization	W	Margules interaction parameter
γ	Activity coefficient	W_G	Regular Margules parameter
γ^∞	Infinite-dilution activity coefficient	$W^{(r)}$	Matrix defined in Eqs. (46)
H	Matrix defined in Eq. (38)	x	Primal GEM speciation (vector)
η	Dual chemical potential	$\hat{x}$	Primal GEM solution (at equilibrium)
I_m	Molal ionic strength	χ	Mole fraction (of a component)
i	Index of stoichiometry unit	X	Matrix defined in Eq. (36)
j	Index of dependent component	y	Vector of experimental data (Eq. (66))
K	Equilibrium constant of reaction	Z	Formula charge (of a component)
L	Set of dependent components	Ξ	Conversion term (Eq. (3))

References

Anderson, G.M., Crerar, D.A., 1993. Thermodynamics in Geochemistry: the Equilibrium Model. Oxford University Press, New York.

Bale, C.W., Pelton, A.D., 1990. The unified interaction parameter formalism: thermodynamic consistency and applications. Metall. Trans., A, Phys. Metall. Mater. Sci. 21A, 1997–2002.

Becker, U., Pollok, K., 2002. Molecular simulations of interfacial and thermodynamic mixing properties of grossular–andradite garnets. Phys. Chem. Miner. 29, 52–64.

Becker, U., Fernandez-Gonzalez, A., Prieto, M., Harrison, R.M., Putnis, A., 2000. Direct calculation of thermodynamic properties of the barite/celestite solid solution from molecular principles. Phys. Chem. Miner. 27, 291–300.

Bethke, C.M., 1996. Geochemical Reaction Modeling: Concepts and Applications. Oxford University Press, New York.

Bischoff, W.D., Bishop, F.C., Mackenzie, F.T., 1983. Biogenically produced magnesian calcite: inhomogeneities in chemical and physical properties; comparison with synthetic phases. Am. Mineral. 68, 1183–1188.

Bischoff, W.D., Mackenzie, F.T., Bishop, F.C., 1987. Stabilities of synthetic magnesian calcites in aqueous solution: comparison with biogenic materials. Geochim. Cosmochim. Acta 51, 1413–1423.

Box, G.E.P., Hunter, W.G., Hunter, J.S., 1978. Statistics for Experimenters: an Introduction to Design, Data Analysis, and Model Building. Wiley, New York.

Busenberg, E., Plummer, L.N., 1989. Thermodynamics of magnesian calcite solid-solutions at 25 °C and 1 atm total pressure. Geochim. Cosmochim. Acta 53, 1189–1208.

Christov, C., 1996. A simplified model for calculation of the Gibbs energy of mixing in crystals: thermodynamic theory, restrictions, and applicability. Collect. Czechoslov. Chem. Commun. 61, 1585–1599.

Christov, C., Petrenko, S., Balarew, C., Valyashko, V., 1994. Calculation of the Gibbs energy of mixing in crystals using Pitzer's model. J. Solution Chem. 23, 795–812.

Curti, E., Kulik, D., Tits, J., 2005. Solid solutions of trace Eu(III) in calcite: thermodynamic evaluation of experimental data over a wide range of pH and pCO_2. Geochim. Cosmochim. Acta 69, 1721–1737.

Filippov, V., Rumyantsev, A., 1990. Application of Pitzer's equations to calculation of solubility diagrams in aqueous–salt systems with continuous solid solution series. Dokl. Akad. Nauk SSSR 315, 659–664.

Gamsjäger, H., 1985. Solid state chemical model for the solubility behaviour of homogeneous solid Co–Mn–carbonate mixtures. Ber. Bunsenges. Phys. Chem. 89, 1318–1322.

Gamsjäger, H., Königsberger, E., Preis, W., 2000. Lippmann diagrams: theory and application to carbonate systems. Aquat. Geochem. 6, 119–132.

Glynn, P.D., 1991. MBSSAS: a computer code for the computation of Margules parameters and equilibrium relations in binary solid-solution aqueous-solution systems. Comput. Geosci. 17, 907–966.

Glynn, P., 2000. Solid solution solubilities and thermodynamics: sulfates, carbonates and halides. In: Jambor, J.L., Nordstrom, D.K. (Eds.), Sulfate Minerals: Crystallography, Geochemistry and Environmental Significance. Rev. Mineral. Geochem., Mineralogical Society of America and Geochemical Society, Washington, D.C., pp. 481–511.

Glynn, P.D., Reardon, E.J., 1990. Solid-solution aqueous-solution equilibria: thermodynamic theory and representation. Am. J. Sci. 290, 164–201.

Glynn, P.D., Reardon, E.J., Plummer, L.N., Busenberg, E., 1990. Reaction paths and equilibrium end-points in solid-solution aqueous-solution systems. Geochim. Cosmochim. Acta 54, 267–282.

Grenthe, I., Plyasunov, A.V., Spahiu, K., 1997. Estimation of medium effects on thermodynamic data. In: Grenthe, I., Puigdomenech, I. (Eds.), Modelling in Aquatic Chemistry. NEA OECD, Paris, pp. 325–426.

Harvie, C.E., Møller, N., Weare, J.H., 1984. The prediction of mineral solubilities in natural waters: the Na–K–Mg–Ca–H–Cl–SO_4–OH–HCO_3–CO_3–CO_2–H_2O system to high ionic strengths at 25 °C. Geochim. Cosmochim. Acta 48, 723–751.

Helgeson, H.C., Delany, J.M., Nesbitt, H.W., Bird, D.K., 1978. Summary and critique of the thermodynamic properties of rock-forming minerals. Am. J. Sci. 278, 1–229.

Herbelin, A.L., Westall, J.C., 1996. FITEQL: a Computer Program for Determination of Chemical Equilibrium Constants from Experimental Data, Report 96-01. Department of Chemistry, Oregon State University, Corvallis, Oregon, pp. 97331.

Hummel, W., Berner, U.R., Curti, E., Pearson Jr., F.J., Thoenen, T., 2002. Nagra-PSI chemical thermodynamic database, version 01/01. Universal Publishers / Upubl.com, New York.

Karpov, I.K., Chudnenko, K.V., Kulik, D.A., 1997. Modeling chemical mass-transfer in geochemical processes: thermodynamic relations, conditions of equilibria and numerical algorithms. Am. J. Sci. 297, 767–806.

Karpov, I.K., Chudnenko, K.V., Artimenko, M.V., Bychinskii, V.A., Kulik, D.A., 1999. Thermodynamic modeling of geological systems by convex programming under uncertainty. Russ. Geol. Geophys. 40, 971–988 (in Russian).

Karpov, I.K., Chudnenko, K.V., Kulik, D.A., Avchenko, O.V., Bychinskii, V.A., 2001. Minimization of Gibbs free energy in geochemical systems by convex programming. Geochem. Int. 39, 1108–1119.

Königsberger, E., 1991. Improvement of excess parameters from thermodynamic and phase diagram data by a sequential Bayes algorithm. Calphad 15, 69–78.

Königsberger, E., Eriksson, G., 1995. A new optimization routine for ChemSage. Calphad 19, 207–214.

Königsberger, E., Gamsjäger, H., 1992a. Comment on "Solid-solution aqueous-solution equilibria: thermodynamic theory and representation" by P. Glynn. Am. J. Sci. 292, 199–214.

Königsberger, E., Gamsjäger, H., 1992b. Solid-solute phase equilibria in aqueous solution: VII. A re-interpretation of magnesian calcite stabilities. Geochim. Cosmochim. Acta 56, 4095–4098.

Kulik, D.A., 2002. A Gibbs energy minimization approach to modelling sorption equilibria at the mineral-water interface: thermodynamic relations for multi-site-surface complexation. Am. J. Sci. 302, 227–279.

Kulik, D.A., Kersten, M., 2001. Aqueous solubility diagrams for cementitious waste stabilization systems: II. End-member stoichiometries of ideal calcium silicate hydrate solid solutions. J. Am. Ceram. Soc. 84, 3017–3026.

Kulik, D.A., Kersten, M., 2002. Aqueous solubility diagrams for cementitious waste stabilization systems: 4. A carbonation model for Zn-doped calcium silicate hydrate by Gibbs energy minimization. Environ. Sci. Technol. 36, 2926–2931.

Kulik, D.A., Kersten, M., Heiser, U., Neumann, T., 2000. Application of Gibbs energy minimization to model early-diagenetic solid-solution aqueous-solution equilibria involving authigenic rhodochrosites in anoxic Baltic Sea sediments. Aquat. Geochem. 6, 147–199.

Kulik, D.A., Dmytriyeva, S.V., Rysin, A.V., Chudnenko, K.V., Karpov, I.K., 2003. GEM-Selektor (GEMS): a Research Program Package for Interactive Thermodynamic Modelling of Aquatic (Geo)Chemical Systems. Waste Management Laboratory, Paul Scherrer Institute. (http://les.web.psi.ch/Software/GEMS-PSI/).

Kulik, D., Berner, U., Curti, E., 2004. Modelling chemical equilibrium partitioning with the GEMS-PSI code. In: Smith, B., Gschwend, B. (Eds.), PSI Scientific Report 2003 / Volume IV. Nuclear Energy and Safety, Paul Scherrer Institute, Villigen, pp. 109–122.

Langmuir, D., 1997. Aqueous Environmental Geochemistry. Prentice Hall, New Jersey.

Lippmann, F., 1977. The solubility products of complex minerals, mixed crystals, and three-layer clay minerals. Neues Jahrb. Mineral. Abh. 130, 243–263.

Lippmann, F., 1980. Phase diagrams depicting aqueous solubility of binary mineral systems. Neues Jahrb. Mineral. Abh. 139, 1–25.

Lippmann, F., 1982. Stable and metastable solubility diagrams for the system $CaCO_3$–$MgCO_3$–H_2O at ordinary temperatures. Bull. Mineral. 105, 273–279.

McCoy, W.H., Wallace, W.E., 1956. Free energies and entropies of formation of KCl–KBr solid solutions at 25 C. J. Am. Chem. Soc. 78, 5995–5998.

Morel, F.M.M., Hering, J.G., 1993. Principles and Applications of Aquatic Chemistry. Wiley Interscience, New York. et al.

Mucci, A., Morse, J.W., 1984. The solubility of calcite in seawater solutions of various magnesium concentrations I_t=0.697 m at 25 °C and one atmosphere total pressure. Geochim. Cosmochim. Acta 48, 815–822.

Nordstrom, D.K., Munoz, J.L., 1994. Geochemical Thermodynamics, 2nd edition. Blackwell Scientific, Palo Alto, CA.

Parkhurst, D.L., Appelo, C.A.J., 1999. User's guide to PHREEQC (version 2)— a computer program for speciation, batch-reaction, one-dimensional transport, and inverse geochemical calculations. U.S.G.S. Water-Resources Investigations Report 99-4259, Denver, Colorado.

Pitzer, K., Kim, J., 1974. Thermodynamics of electrolytes: IV. Activity and osmotic coefficients for mixed electrolytes. J. Am. Chem. Soc. 96, 5701–5707.

Prieto, M., Fernandez-Gonzalez, A., Becker, U., Putnis, A., 2000. Computing Lippmann diagrams from direct calculation of mixing properties of solid solutions: application to the barite–celestite system. Aquat. Geochem. 6, 133–146.

Urusov, V.S., 1975. Energetic theory of miscibility gaps in mineral solid solutions. Fortschr. Mineral. 52, 141–150. (Spec.Issue).

Vinograd, V.L., 2001. Configurational entropy of binary silicate solid solutions. In: Geiger, C.A. (Ed.), Solid Solutions in Silicate and Oxide Systems of Geological Importance. EMU Notes in Mineralogy. Eötvös University Press, Budapest, pp. 303–346.

Wood, B.J., Nicholls, J., 1978. The thermodynamic properties of reciprocal solid solutions. Contrib. Mineral. Petrol. 66, 389–400.